DEFENCE R&D DÉFENSE

QWIP-LED/CCD Coupling Study: Final Report

Shen Chiu
Defence Research Establishment Ottawa

Al Scott
EMS Technologies

Defence R&D Canada
DEFENCE RESEARCH ESTABLISHMENT OTTAWA

TECHNICAL REPORT
DREO TR 2000-101
November 2000

National Defence Défense nationale

Canada

DEFENCE R&D DÉFENSE

QWIP-LED/CCD Coupling Study: Final Report

Shen Chiu
Space Systems Group
Space Systems and Technology Section

Al Scott
EMS Technologies

DEFENCE RESEARCH ESTABLISHMENT OTTAWA

TECHNICAL REPORT
DREO TR 2000-101
November 2000

Project
5EF12

Abstract

Many space-based imaging applications demand a sensitive, low noise long wavelength IR detector which is able to image a wide field of view in a short time. Quantum Well Infrared Photodetector (QWIP)-LED detectors offer the potential for large imaging area, and ultra-low noise operation when cooled to cryogenic temperatures (~30K). Due to these factors the QWIP-LED holds a significant advantage over conventional detectors. It is in the area of system efficiency, however, that current QWIP-LEDs are less competitive for low signal space applications. This study was a collaborative effort between EMS technologies, DND, CRESTech and NRC with a goal to design and implement a method to increase the efficiency of QWIP-LED systems.

As a result of this study, it has become apparent that early projections about the cost, quality, and efficiency of pixelless QWIP-LED technology were highly optimistic regarding critical implementation details. Unforeseen difficulties with the application of 'standard' LED and grating technologies to a non-standard device severely impacted the predicted efficiency for both absorption and emission.

EMS' research into the IR detector market allowed realistic comparisons to be made for expected applications and showed that, in the near term and at the current rate of development, the QWIP-LED would not be an easily manufacturable competitive alternative due to cryogenic cooling requirements, unexplained material defects, and overall low efficiency. The competing QWIP-multiplexer which is now commercially available would have identical noise and cooling specifications with much higher efficiency at a comparable cost. Uncooled bolometric detectors would compete favourably for high signal terrestrial and earth-observing markets while at the high performance end, more efficient thin film HgCdTe detectors can now cover most wavebands of interest with much higher efficiency, thus out-competing QWIP-LED for space applications.

Résumé

De nombreuses applications d'imagerie spatiales exigent un détecteur IR sensible à grande longueur d'onde et à bruit réduit capable de générer en peu de temps une image à large champ de vision. Les détecteurs QWIP-DÉL offrent le potentiel d'une grande surface d'imagerie et d'un fonctionnement à bruit extrêmement réduit lorsqu'ils sont refroidis à des températures cryogéniques (~30 K). Vu ces facteurs, le QWIP-DÉL a un avantage considérable par rapport aux détecteurs classiques. C'est au niveau du rendement du système, cependant, que les QWIP-DÉL actuels sont moins compétitifs dans le cas des applications spatiales à signaux faibles. Cette étude était un effort de collaboration entre EMS Technologies, le MDN, CRESTech et le CNRC ayant pour objectif de concevoir et de mettre en œuvre une méthode pour augmenter le rendement des systèmes à photodétecteur infrarouge à puits quantique et à diode électroluminescente (QWIP-DÉL).

Au cours de cette étude, il s'est avéré que les projections initiales du coût, de la qualité et du rendement de la technologie du QWIP-DÉL sans pixel avaient été fort optimistes à l'égard des détails critiques de mise en œuvre. Des difficultés imprévues dans l'application des technologies « standard » des DÉL et des réticules à un dispositif non standard ont nui grandement au rendement prédit tant pour l'absorption que pour l'émission.

La recherche d'EMS sur le marché des détecteurs IR a permis de faire des comparaisons réalistes pour des applications prévues, lesquelles ont montré que, à court terme et au rythme de développement actuel, le QWIP-DÉL ne serait pas une solution de rechange de fabrication facile et compétitive à cause des exigences de refroidissement cryogénique, des défauts de matériaux sans explication et du faible rendement global. Le multiplexeur QWIP compétitif, qui est maintenant vendu dans le commerce, aurait des caractéristiques de bruit et de refroidissement identiques avec un rendement beaucoup plus élevé et ce, à un coût comparable. Les détecteurs bolométriques gagneraient la compétition sur les marchés des détecteurs terrestres et d'observation de la Terre à signaux forts, tandis que, dans le haut de gamme, des détecteurs HgCdTe à couche mince plus efficaces couvrent maintenant la plupart des gammes d'ondes d'intérêt avec un rendement nettement supérieur, l'emportant ainsi sur les QWIP-DÉL pour ce qui est des applications spatiales.

Executive summary

The low quantum efficiency of current QWIP-LED/CCD systems was identified by the previous EMS applications study as a major impediment to successful space applications and competitive terrestrial and airborne exploitation of this emerging technology. In the current study, high efficiency QWIP-LED to CCD coupling schemes were investigated by EMS in collaboration with DND, CRESTech and NRC. A manufacturable solution was found, utilizing EMS expertise in optical systems and CCD technology and a study was devised to test the resulting design.

It was predicted that a total system quantum efficiency (QE) of ~15% would be necessary for successful space applications, while a value of ~10% would allow competitive use in airborne and terrestrial applications. These numbers, low relative to standard HgCdTe IR detectors (>70% QE), were thought to be acceptable due to the perceived ease of fabrication and low cost of a pixelless quantum well device. During the course of the study it was determined that the original predictions would not be reached in the timescale of the current program due to unforeseen difficulties in the practical application of this new technology. The following table illustrates the current status of the QWIP-LED/CCD efficiency compared to previous and near future (~2 yrs) expectations.

Table 0-1 End to End Quantum Efficiency of QWIP-LED/CCD Device

Detector Stage	Predicted QE	Current QE	Foreseeable QE
QWIP IR absorption	50%	$\leq$ 0.5%	4%
LED conversion	100%	75%	90%
LED to Faceplate Coupling	100%	N/A	25%
Faceplate Transfer	50%	53%	55%
CCD detection	60%	4%	40%
Total QE	**15%**	**N/A**	**0.20%**

Space applications of the device are ruled out due to the low QE, while terrestrial markets will be expected to be dominated by bolometric IR detectors with similar efficiencies which do not require cryogenic cooling like the QWIP. It has become apparent that the complexity of the QWIP-LED manufacturing process, due in part to unforeseen material defects, will be similar to that of direct-bonded QWIP-multiplexers already being successfully implemented with higher QE by competing groups. Because of the foreseeable QE of the QWIP-LED device as revealed by this study, and ongoing practical difficulties in fabricating a working QWIP-LED, it has been mutually decided amongst the collaborating institutions to discontinue the project.

Although the primary goal of the study was not achieved, the work done to this point has been of significant value to all parties involved. EMS and CRESTech have gained useful expertise in cryogenic CCD operation and readout. NRC staff have gained highly

marketable experience in semiconductor manufacturing techniques, and DND will be able to apply this result in order to redirect research funding to more promising alternatives.

Scott, A., Chiu, S. 2000. QWIP-LED/CCD Coupling Study. DREO TR 2000-101. Defence Research Establishment Ottawa.

Sommaire

Le faible rendement quantique des systèmes QWIP-DÉL/DTC a été identifié par l'étude précédente des applications d'EMS comme un des obstacles principaux aux applications spatiales et à l'exploitation terrestre et aérienne compétitive de cette technologie émergente. Dans le cadre de la présente étude, des systèmes de couplage du QWIP-DÉL au DTC à haut rendement ont été étudiés par EMS, conjointement avec le MDN, CRESTech et le CNRC. On a trouvé une solution permettant la fabrication, qui fait appel à la compétence d'EMS en systèmes d'optique et en technologie des DTC, et l'on a conçu une étude pour tester la réalisation qui en a résulté.

Il a été prédit qu'un rendement quantique (QE) de l'ensemble du système de ~15 % serait nécessaire pour des applications spatiales efficaces, tandis qu'un rendement de ~10 % permettrait l'utilisation compétitive dans les applications aériennes et terrestres. Ces chiffres, bien que faibles comparativement à ceux des détecteurs IR standard au HgCdTe (QE > 70 %), étaient jugés acceptables en raison de la facilité de fabrication apparente et du coût réduit du dispositif à puits quantique sans pixel. Au cours de cette étude, on a déterminé que les prédictions originales ne seraient pas réalisées dans le délai du programme actuel à cause de difficultés imprévues dans la mise en œuvre pratique de cette nouvelle technologie. Le tableau ci-dessous illustre l'état actuel du rendement du QWIP-DÉL/DTC comparativement aux attentes précédentes et à court terme (~2 ans).

Tableau 0-1 Rendement quantique de bout en bout du dispositif QWIP-DÉL/DTC

Étage du détecteur	QE prédit	QE actuel	QE prévu
Absorption IR du QWIP	50 %	$\lesssim$ 0,5 %	4 %
Conversion DÉL	100 %	75 %	90 %
Couplage DÉL - plaque avant	100 %	S/O	25 %
Transfert de plaque avant	50 %	53 %	55 %
Détection DTC	60 %	4 %	40 %
QE total	**15 %**	**S/O**	**0,20 %**

Les applications spatiales du dispositif sont éliminées à cause du faible QE, tandis qu'on s'attend à ce que les marchés terrestres seront dominés par les détecteurs IR bolométriques à rendements semblables qui n'exigent pas de refroidissement cryogénique, au contraire du QWIP. Il s'est avéré que la complexité du procédé de fabrication du QWIP-DÉL, due partiellement à des défauts imprévus des matériaux, sera semblable à celle des multiplexeurs à QWIP à raccordement direct et à QE supérieur déjà mis en œuvre par des groupes de compétiteurs. Compte tenu du QE prévu du dispositif QWIP-DÉL, tel que révélé par la présente étude, et des difficultés pratiques permanentes à fabriquer un QWIP-DÉL fonctionnel, il a été décidé d'un accord commun parmi les organisations collaboratrices de discontinuer le projet.

Bien que l'objectif principal de l'étude n'ait pas été atteint, le travail effectué jusqu'ici a été d'une valeur considérable pour toutes les parties. EMS et CRESTech ont acquis une compétence utile en matière de fonctionnement et d'affichage des DTC cryogéniques. Le personnel du CNRC a acquis une expérience très commercialisable en matière de techniques de fabrication de dispositifs à semiconducteurs, et le MDN sera en mesure de mettre en valeur ce résultat afin de réacheminer le financement de la recherche vers d'autres projets plus prometteurs.

Scott, A., Chiu, S. 2000. QWIP-LED/CCD Coupling Study: Final Report. DREO TR 2000-101. Centre de recherches pour la défense Ottawa.

Table of contents

Abstract i

Résumé ii

Executive summary iii

Sommaire v

Table of contents v

List of figures x

List of tables xi

1 Introduction 1

2 Background 3

3 Results by Task 7

3.1 QWIP-LED Research at NRC 7

3.1.1 QWIP-LED Philosophy 7

3.1.2 Principle of Operation 7

3.1.3 Reflective QWIP-LED devices 7

3.1.4 Rationale of Transmissive QWIP-LED Geometry: 8

3.2 QWIP-LED Optimization at NRC 10

3.2.1 V-Groove Influence on LED Emission 10

3.2.2 Attenuation at V-groove Facets 10

3.2.3 Photon Recycling 10

3.2.4 Top and Bottom Coatings 12

3.2.5 Material Defects 12

3.2.6 Substrate Removal Process 13

3.2.7 CONCLUSIONS 15

3.3 QWIP-LED/CCD Optimization Research at EMS 16

3.3.1 Substrate Materials/Compatibility 16
3.4 Analysis of Options/Tradeoffs 17
3.4.1 Direct Bonding/Fiber Optic Faceplate 17
3.4.2 Microgap 20
3.4.3 Non-Traditional Optical Solutions 21
3.5 Bonding of Test Samples and Assembly Procedure 22
3.6 Testbed Design and Fabrication at CRESTech 23
3.7 Test Procedure 23
3.7.1 Charge Transfer Efficiency 23
3.7.2 Responsivity 24
3.8 Acquisition and Characterization of CCDs 24

4 Lessons Learned 32

5 Conclusions 33

References 34

Appendix A 35
A.1 SCOPE 35
A.2 INTRODUCTION 35
A.3 REFERENCE DOCUMENTS 35
A.4 PROBLEM DEFINITION 35
A.5 ASSUMPTIONS 36
A.6 CALCULATIONS 36
A.7 DISCUSSION 38
A.8 CONCLUSIONS 38

Appendix B 39
B.1 Assemble Fiber-Optic/CCD Bonding Jig 39
B.2 Pre-Set Testing 39
B.3 Adhesive Screening Test 39

Appendix C 42
C.1 Thermal Analysis Procedure 42
C.2 Results 42

List of symbols/abbreviations/acronyms/initialisms 47

Distribution list 48

List of figures

Figure 2-1 Schematic illustration of a QWIP-LED device 4
Figure 2-2 System size comparison 6
Figure 3-1 Sketch of V-groove transmissive QWIP design 9
Figure 3-2 Image transfer blurring contributions for direct bond design 19
Figure 3-3 Fiber optic faceplate design 19
Figure 3-4a Fiber optic direct bond design for QWIP-LED/CCD coupling 21
Figure 3-4b Fiber optic direct bond design for QWIP-LED/CCD coupling 22
Figure 3-5 Cryogenic CCD testbed at CRESTech 23
Figure 3-6 Quantum efficiency vs. wavelength for different CCD types 24
Figure 3-7a 0-300 K temperature vs. signal loss due to CTI of SBC CCD 25
Figure 3-7b Measured CTI vs. temperature for Dalsa CCDs 26
Figure 3-8 Background signal vs. temperature and waveband for QWIP-LED 27
Figure 3-9a Signal loss due to CTI vs. temperature and pixel clock period 28
Figure 3-9b Measured signal loss vs. transfer rate at 85 K 28
Figure 3-10a Shift in red responsivity due to cryogenic cooling of CCD 29
Figure 3-10b Measured shift in CCD responsivity vs. temperature and wavelength 30
Figure 3-11 Measured responsivity of CCD vs. wavelength at 296 K 31
Figure A-1 Schematic of the substrate/faceplate interface 35
Figure C-1 QWIP-LED/CCD thermal analysis results 44
Figure C-2 Thermal analysis results for QWIP-LED only 45
Figure C-3 Thermal analysis results for CCD surface only 46

List of tables

Table 0-1 End-to-end Quantum efficiency of QWIP-LED/CCD device..... iii

Table A-1 CTE data for applicable materials 36

Table A-2 Data for potential adhesives 36

Table B-1 Results of adhesive bonding trials 40

1. Introduction

This study was a collaborative effort between EMS technologies, DND, CRESTech and NRC with a goal to design and implement a method to increase the efficiency of quantum well infrared photodetector (QWIP)-LED systems. QWIP-LEDs have recently been developed at NRC by H.C. Liu *et al.* (1995) for mid- to long wavelength infrared (≥3μm) imaging applications. The QWIP-LED acts as a frequency up-converter by absorbing long wavelength infrared (IR) photons, and re-emitting them in the near infrared (NIR) where they can be subsequently imaged by a conventional CCD camera.

The purpose of the study was to improve the transfer efficiency of these intermediate NIR photons from the LED to the CCD while maintaining reasonable image integrity. In simple device geometry only a small fraction of the photons (~2%) emitted in the LED layer will escape into the air without being reflected from the interface. This is because of the high refractive index of the LED material as compared to that of air. Several possibilities exist to improve this situation including anti-reflection (AR) coatings, index-matching transfer materials, and reflective backing of the thin LED layer. Once this transmission barrier has been overcome, conventional optics are only able to capture a small portion (~10%) of these escaping photons and redirect them to the CCD for final imaging. The rest of the NIR photons are emitted at wrong angles and end up missing the lens entirely. Using more powerful optics, a larger fraction of the signal can be transferred, but the quality of the resulting image will be severely degraded by aberrations. By fully exploring emerging technologies such as microlens arrays, gradient index or diffractive optics and fibre-optic couplers, it was thought possible to increase this intermediate stage to nearly 50% efficiency, while maintaining a sharp, high resolution image.

We attempted to solve the coupling problem by designing, fabricating and testing non-standard imaging solutions which give improved efficiency without significantly impacting the image quality. This study was aimed to provide a convincing test to demonstrate whether a QWIP-LED/CCD detector should be considered for stringent low signal IR imaging applications. For high signal earth and atmospheric observations, both the QWIP-LED and the CCD may operate at 77K to achieve low noise levels. For long wavelength or low signal observations, the QWIP-LED must operate at lower temperatures ~30K to improve the signal to noise ratio. The CCD must be held at or above ~60K to operate correctly.

Preliminary research indicated that the coupling scheme should consist of direct bonding, fibre-optic faceplates, advanced optics and/or micro-gaps. Direct bonding of the QWIP-LED to the CCD is the most efficient possibility for an IR imaging detector. This is similar to the solution being pursued by other QWIP research groups in which a pixellated QWIP is bonded directly to a silicon readout multiplexer. Many difficulties must be overcome to make direct bonding feasible including material

incompatibility, interface reflections and photonic spreading. Fibre-optic faceplates allow channeling of photons with very high resolution, high numerical aperture, and little absorption loss. These faceplates have already been used by EMS to transfer images in similar applications. The high numerical aperture allows the faceplate to capture a large proportion of the incoming photons, allowing for a high transfer efficiency.

Fabrication of microlens arrays was considered as a transfer option in the preliminary research. Other advanced optical solutions include the newly emergent technology of diffractive optics, and the recently commercialized option of gradient index optics. These techniques potentially allow imaging at much higher light collecting efficiencies than standard technologies. The design of a microscopic mechanical gap was considered to eliminate problems associated with heat transfer and thermal stress. By keeping the gap extremely small (less than one pixel) the space available for the signal photons to disperse will be minimized. Each solution has various technological and engineering challenges associated with its implementation, which will be discussed in this report.

EMS, in collaboration with DREO, CRESTech, and NRC researched the best potential coupling schemes and then designed an experiment to test the efficiency of the most promising candidate. NRC attempted to fabricate the necessary solid state QWIP-LEDs. The efficiency measurements were to be carried out in a cryogenic evacuated testbed at the CRESTech characterization facility.

2. Background

Many space-based imaging applications demand a sensitive, low noise long wavelength IR detector which is able to image a wide field of view in a short time. QWIP-LED detectors offer the potential for large imaging area, and ultra-low noise operation when cooled to cryogenic temperatures (~30K). Due to these factors the QWIP-LED holds a significant advantage over conventional detectors. It is in the area of system efficiency, however, that current QWIP-LEDs are less competitive for low signal space applications. At present, less than 1% of incoming photons can be measured by prototype QWIP-LED systems. The recent QWIP-LED Application and Cost Estimate Study performed by EMS under contract to DREO investigated the imaging of distant objects in a low background environment. The study indicated that the low efficiency of the LED to CCD link was a crucial factor in the resulting system size, complexity and cost. The present study was proposed as a follow-up to overcome the photonic coupling problem and to generate a competitive advantage over existing IR detector technology.

The QWIP-LED is a pixelless device that can be tuned to transform a particular wavelength of IR photons into photons that can be detected by a CCD. Because it is fabricated as a stack of thin GaAs

Commercial Space Applications

1. Resource Monitoring
   - -Forest Fire Detection
   - -Crop Health Monitoring
   - -Agriculture Inventory
2. Atmospheric Science
   - -Atmospheric Temperature Monitoring
   - -Atmospheric Wind Monitoring
   - -Atmospheric Chemistry / Pollution Monitoring
   - -Cloud Detection
3. Terrestrial Science
   - -Mineral Detection
   - -Surface Temperature Monitoring
4. Ocean Sciences
   - -Ocean Temperature Monitoring
   - -Ocean Current Monitoring
5. Astronomy
   - -IR Sky Mapping
   - -Asteroid/Meteorite Detection / Tracking
6. Planetary Sciences
   - -Surface Mapping
   - -Surface Temperature
   - -Surface Chemistry

Military Space Applications

7. Space Defence
   - -Missile Detection & Tracking
   - -Space Debris Detection & Tracking
8. Air Defence
   - -Aircraft Detection & Tracking
9. Terrestrial Surveillance
   - -Detection & Tracking of Vehicles
10. Ocean Surveillance
    - -Ship Detection

layers, the construction of the detector avoids the extra labour associated with pixellation masks during the microfabrication phase. As well, the heat load on the QWIP-LED is diminished because the heat-generating readout circuitry is all located within the CCD. Only a few very thin current carrying wires are necessary for biasing. This allows the crucial low band-gap detection stage to be cooled to much lower levels than would otherwise be possible, giving the option of a very low noise system. A schematic of a QWIP-LED is shown in *Figure 2-1*. Because this is such a new technology, not much research has been done on the practical details of incorporating this detector into a useable system.

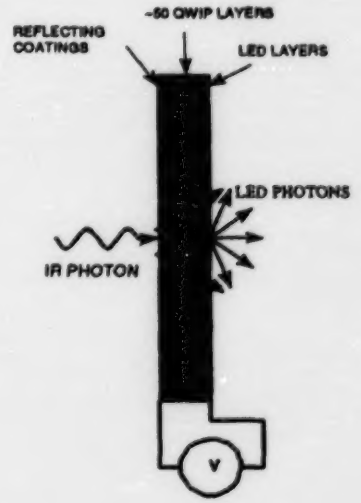

Figure 2-1

Schematic illustration of a QWIP-LED device

Pursuant to the EMS QWIP-LED Application and Cost Estimate Study, a need for increased detection efficiency of existing QWIP-LED systems was identified. Currently the QWIP-LED developed by H.C. Liu's group at NRC emits NIR photons which are reimaged through standard optics onto a CCD detector. Pre-study estimates of achievable QWIP photon to electron conversion efficiency (quantum efficiency) were set at ~50%, with corresponding CCD quantum efficiency (QE) of 40%. With an f/1 optical system, and diffuse emission from a flat surface, a total system efficiency of ~2.1% is the maximum achievable. This ignores the problem of getting the light out of the high index LED region of the QWIP-LED through a high-contrast interface. This relatively small quantum efficiency is a severe drawback for any low signal application such as often encountered in space-based work. High quality HgCdTe IR detectors can operate with QEs of ~70%. To make the QWIP-LED an attractive option in the same spectral region, an increased system efficiency is necessary. By replacing the standard reimaging optics with a more efficient coupling scheme (see Figure 2-2), it was thought possible to increase the overall QE to perhaps 15%.

Ease of Fabrication

Because the QWIP-LED is a pixelless device incorporating no internal circuitry, the fabrication process is nearly as easy as depositing a multi-layer optical coating. No photolithography or micro-etching is necessary. This means that the equipment necessary for production is relatively uncomplicated, and the expense and difficulty associated with the indium bump bonding of standard IR detectors is avoided.

The QWIP-LED is a pixelless device which relies on mature and proven deposition technologies to fabricate the necessary high quality layered GaAs films. The use of such a well studied material as the basis for a detector provides the advantage of low impurity-based dark current. At temperatures below 50K, QWIP-LED dark current is better than that of HgCdTe detectors. In addition to this, the deposition techniques available can be expanded to create much larger detector areas with higher uniformity than other available devices. Due to uniformity difficulties, HgCdTe detectors are usually only ~1cm square. It was thought that high performance transmissive QWIP-LEDs would be readily producible in sizes up 2 cm on a side. Multi-colour devices were also hypothesized with up to 100% fill factor temporally as well as spatially in both colours. QWIP-LED devices are possibly unique in this aspect, allowing one to observe photons in two or more different wavebands with a single detector at the same time without loss of resolution. This can be useful for many applications, providing thermal discrimination of targets and offering the possibility of clutter rejection with a minimum of complex image processing. The LED aspect to the NRC detector allows the added advantage of utilizing mature silicon-based CCD readout technology which presently comes at the expense of decreased system efficiency. CCD readouts give one the option of multiple on-chip binning schemes including time domain integration (TDI). These strategies allow longer integration times for scanning detectors, decreasing the relative noise contributions of the readout stage. Due to the intrinsic advantages of CCD technology over standard HgCdTe MUX readouts, as well as the multi-spectral capabilities of the QWIP, a QWIP-LED with a QE of even 10% would be a competitive alternative for many applications.

Particular QWIP-LED applications which have been previously identified in the EMS Application study include SBIRS low and debris tracking where the large area and TDI advantages would allow full sky coverage if an increased coupling efficiency were available. The multispectral ability combined with tunability to long wavelengths would allow discrimination of targets with varying temperatures and the detection of cooled objects. The low dark current combined with the large area would be of great use to astronomical applications, if the efficiency problem could be overcome.

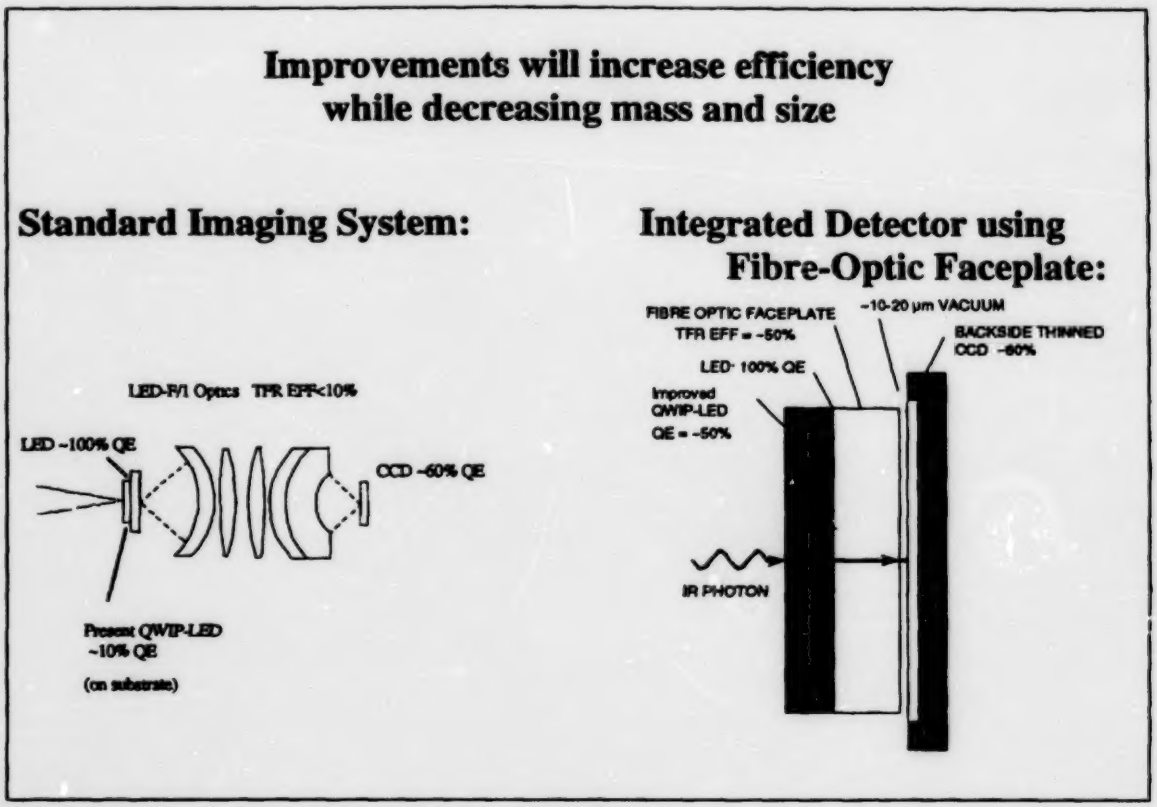

Figure 2-2 *System size comparison*

3. Results by Task

3.1 QWIP-LED Research at NRC

3.1.1 QWIP-LED Philosophy

An important philosophy of the QWIP-LED approach to infrared imaging is the use of all mature and well-established technologies. This hopefully will lead to cheaper detectors. Other advantages include the elimination of hybridization integration with a Si readout circuit (the traditional approach), the implementation of a pixelless imaging device with reduced fabrication steps, and the possibility of fabricating very large area sensors.

3.1.2 Principle of Operation

A Quantum Well Infrared Photodetector (QWIP) is epitaxially integrated with a light emitting diode (LED). The device (QWIP-LED) is operated under a constant forward bias high enough to turn on the LED. Upon far/mid infrared illumination the resistance of the photoconductor (i.e. QWIP) is decreased and, thus, an additional voltage is applied across the LED which leads to an increase of the near infrared emission of the LED. The result is an up-conversion of a far/mid infrared signal to a near infrared signal. The near infrared output can then be imaged by a well developed device such as Si Charge-Coupled Device (CCD) camera.

3.1.3 Reflective QWIP-LED devices

The first attempt to implement the QWIP-LED imaging was based on the so-called reflective QWIP-LED configuration [1], in which both the incident far/mid infrared light and the LED near infrared output are on the front side of the device. The optics for this mode of operation is inherently more complicated and less efficient. Also, the far/mid infrared light coupling to quantum wells requires transmission grating structures that are more difficult to fabricate or V-groove coupling schemes which rely on refraction of the incident far/mid infrared radiation—a rather inefficient coupling method. As the incoming far/mid light impinges on a V-groove facet, the light is refracted into an angle 57° from the optimum coupling angle (i.e., 90° with respect to the incident light or parallel to the quantum wells). In addition, to minimize image smearing it was necessary to use a n^+ GaAs substrate to absorb the far/mid infrared light as it exits the active region of the QWIP in order to avoid reflection at

the GaAs/air interface on the bottom of the substrate. This is due to the fact that the reflective QWIP is not back-thinned, and back-surface reflections could end up being detected a significant distance from where the light entered the device. For this same reason, the GaAs substrate would also absorb all of the LED light emitted in the direction of the substrate. With the absorbing substrate and the small escape cone, only ~2% of the near IR light is emitted externally.

3.1.4 Rationale of Transmissive QWIP-LED Geometry

Both the QWIP absorption quantum efficiency and the LED external efficiency can be significantly improved by operating the QWIP-LED in the transmissive mode. That is, the incoming far/mid infrared light is incident on one side of the device and the resulting near infrared image is output at the other side. This mode of operation, however, requires that the GaAs substrate be completely removed.

The absorption QE of the QWIP is also expected to improve because the transmissive configuration uses a reflective V-groove geometry ([2] see Figure 3.1) as opposed to the transmissive or refractive V-groove geometry. In this configuration, a 45° V-groove facet reflects the incident M/FIR light into the optimum coupling angle (i.e., exactly parallel to the QWs). Depending on the ratio of the V-groove coverage area to the total imaging area ("fill factor") and assuming strong far/mid infrared absorption, this coupling scheme can, at best, improve the QWIP absorption QE up to 50% (i.e., 100% coupling of the TM component of the incident light). This is because of the one-dimensional nature of the V-grooves. Typical V-groove far/mid infrared light coupling efficiencies using a V-groove structure are in the order of 10 to 15 % [2].

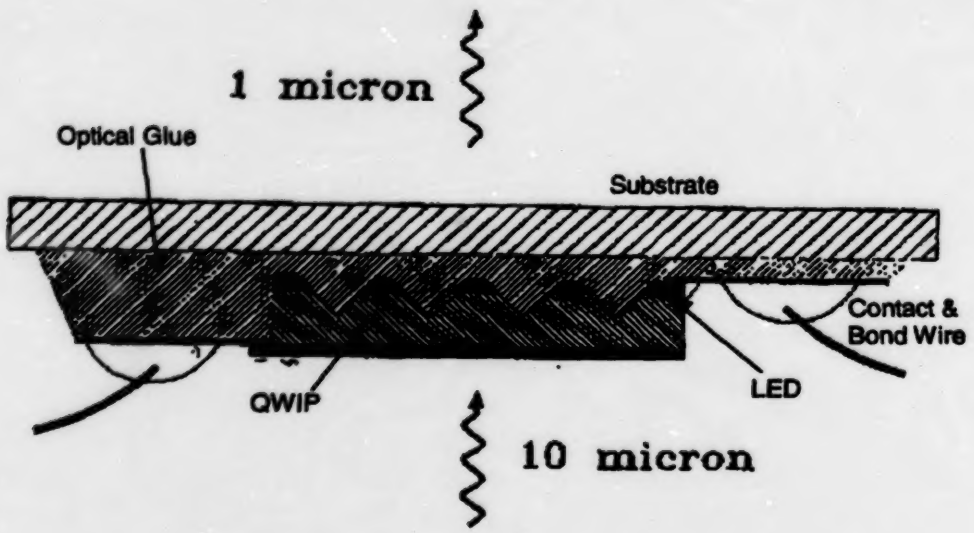

Figure 3-1 Sketch of V-groove transmissive QWIP design.

The coverage area of the V-grooves (i.e., the number of V-groove facets) can be increased without destroying the LED active area by first growing the LED layer and then the QWIP layer. This may be more advantageous in that the LED light can now escape through two escape cones (i.e., via the two 45° facets) rather than only through the highly doped top contact layer (with additional free carrier absorption losses). The reduction in the sheet resistance can be compensated for by higher doping of the top contact layer or by depositing a metallic grid on the remaining flat top surfaces.

Furthermore, two-dimensional (2-D) reflective gratings, capable of coupling both components of the incident radiation, instead of V-grooves can be used to improve the QWIP absorption QE. These have been the subject of intensive studies. An impressive absorption QE of 92% has been achieved by Andersson and Lundqvist [3] using a waveguide with a doubly periodic grating coupler. We have also evaluated various 2-D reflective grating designs. The 2-D grating structures are expected to be less susceptible to device cleavage problems than the V-groove ones due to substrate thinning, but their coupling efficiency may be more difficult to model or to predict.

3.2 QWIP-LED Optimization at NRC

3.2.1 V-Groove Influence on LED Emission

Recent results on V-grooved QWIP-LEDs showed that wet-etching a V-groove structure through the LED active region led to considerably lower electro-luminescent (EL) emissions of the LED [4]. The effect was attributed to non-radiative recombination at surface states on unpassivated V-groove facets. This difficulty can be overcome by growing the QWIP on top of the LED, thus avoiding etching V-grooves through the LED region. A wafer with this "up-side-down" structure has been grown (opposite of Figure 3.1 LED orientation). Device fabrications and tests are being planned. Other solutions such as surface passivation were also proposed. Initial passivation experiments on GaAs samples, by Prof. Z.H. Lu of University of Toronto, showed positive results. Experiments with a "real" V-grooved QWIP-LED device are in progress. On the other hand, using the 2-D grating coupler is less intrusive and allows the LED to be grown either on top of or below the QWIP without affecting the LED performance. Experimental results showed that LED emissions were not affected by reactive-ion etching (RIE) a 2-D grating structure on top of the QWIP-LED [4].

3.2.2 Attenuation at V-groove Facets

It was shown that far/mid infrared light internally reflected at V-groove facets is partially absorbed in the optical glue due to the fringing optical field. Even though the far/mid light undergoes total internal reflection at the 45° V-groove facet, the optical electrical field in fact extends beyond the GaAs/glue interface. A MgF_2 thin film was proposed as a non-absorbing layer to be deposited in between the V-groove facet and the glue to minimize the fringing effect. First results showed that a 0.75 μm thick MgF_2 film was sufficient to eliminate most of the glue-absorption problem. A slightly thicker layer will be used for the final design to completely avoid the absorption in the glue.

3.2.3 Photon Recycling

In order to achieve high detector sensitivity, it is important to optimize the QWIP-LED output, which depends on the external quantum efficiency (QE) of the integrated LED. The internal QE of III-V double heterostructure LED can be well over 90% [5]. However, this high internal yield must be converted into useful external output. In general, the external QE of LEDs is rather poor, typically only a few percent. The reason for this low output is that the semiconductor refractive index is rather high (n ~ 3.54 in GaAs), leading to a very narrow escape cone for the isotropic spontaneous

emission of NIR light from GaAs into air. The 16° half cone angle imposed by Snell's Law covers a solid angle of only ~ $(1/4n^2)\times 4\pi$ steradians. For GaAs this translates into an external efficiency of ~2%.

To increase the external efficiency of the LED, one possible technique is to make use of re-absorption and re-emission (i.e., recycling) of the LED photons. At each emission or re-emission, 2-4 % of the total LED light escapes from the high index material. After many re-incarnation events, a high LED output (or external efficiency) can be achieved. In order to minimize image smearing, the substrate must be removed and the LED active layer must be thick. This process takes advantage of the nearly 100% internal efficiency of the LED. The external efficiency was shown to be very sensitive to any loss in the microcavity. A model calculation [6] has shown that for a substrate-removed transmissive QWIP-LED device with a thick LED active layer (~6000 Å), the LED external efficiency can be increased up to ~15 % by recycling the trapped LED photons and capturing the escaped LED light using a fiber optic faceplate. The image smearing due to photon lateral spreading can be kept within ~30 μm. Even higher efficiencies (> 80 %) with negligible image smearing can be achieved by directly bonding the QWIP-LED to a Si CCD chip. However, the latter may be frustrated by temperature nonuniformity of the CCD imaging chip — since QWIP detectivity is very sensitive to temperature variation — and its poor charge transfer efficiency at cryogenic temperatures.

Experimental results have shown, however, that the thick LED layer led to a significant drop in the LED internal efficiency, which translated into a low external efficiency (~0.25% without photon recycling) in the current regime that the QWIP-LED normally operates (~1 mA/cm^2). This was attributed to an increase in carrier diffusion lengths. With the thick LED active region, electrons and holes would have to travel much further before recombination, and this process would occur with lower probability than in the case of a quantum-well type LED. One proposed solution to this problem was to dope the LED active layer with Be in order to enhance the recombination process. With a Be doping of ~3×10^{16} cm^{-3} and a LED active layer thickness of 4000 Å, the result showed an improvement in external efficiency from 0.25 % to 1.5 % (without recycling), which translated to an internal efficiency of ~70 %. This was not at all satisfactory since previous simulation results demonstrated that the effectiveness of the photon recycling was very much dependent on the LED internal efficiency. However, more work is being planned to further optimize the doping of the LED active region.

The other proposal put forward was to have a separate thick photon recycling layer outside of either the top or the bottom contact, while the LED active layer was kept at 300 Å to ensure a very high internal QE. After the initial LED emission in the 300 Å layer, all subsequent re-absorption and re-emission events take place mostly in the thick photon recycling layer. This approach guarantees both efficient photon recycling

and a high LED internal efficiency. A wafer incorporating this new design structure has not yet been grown. No schedule has yet been set for the wafer growth.

3.2.4 Top and Bottom Coatings

The designs of top and bottom mirror coatings turned out to be much more challenging than originally anticipated. In particular, the top coating for the 2-D grating coupler structure would have to be completely reflective at far/mid infrared (F/MIR) and completely transmissive at near infrared (NIR). Any loss due to an imperfect reflection at F/MIR or a poor transmission at NIR would result in a poor QWIP absorption QE and a low LED external efficiency, respectively. The current design is a thin gold film varying from 50 to 100 Å in thickness. A 100 Å Au film was calculated to have a 50 % transmission and a 7.5 % absorption loss at NIR and a 75 % reflection at F/MIR. Similar performance was also found for silver thin films. The top mirror is not essential, however, when using a V-groove structure as the F/MIR coupler. Due to the large difference in refractive index between GaAs and air (or MgF_2), the incoming F/MIR light would be completely reflected at the interface.

For the bottom coating, the requirements are similar to those of the top coating. The thin film would have to be transmissive at F/MIR and reflective at NIR. The bottom coating is particularly important as a mirror at NIR to promote photon recycling in the microcavity. Presently, the proposed coating is a ThF_4/ZnSe multi-layer dielectric film of ~1.1 μm thickness. No test results are yet available at the moment. The biggest concern with this type of film is thermal mismatch with the host material GaAs. Its relatively thick coating (about a third of the total thickness) would only compound the problem. Our previous experience with a dielectric coating (for top coating) resulted in cracking of the film when submerged in liquid nitrogen.

3.2.5 Material Defects

3.2.5.1 Laser ablation

The presence of bright electroluminescent spots caused by the draining of electrical current via crystallographic defects are particularly detrimental to a pixelless QWIP-LED device because the good and the defective areas on the device are interconnected. This extra connectivity means that a single bad defect could potentially shunt the rest of the device, rendering it inoperative. Femtosecond laser ablation was shown to be a very convenient and precise technique to remove or isolate these defects.

The principle of femtosecond laser ablation is to etch a square trench around the crystallographic defect in order to electrically isolate it from the rest of the device. It was shown that a complete isolation of a deeply buried defect would require typically a ~2 μm deep etch into the device. The required etch depth appeared to depend on how deep these defects were buried underneath the surface. Atomic Force Microscope (AFM) showed that one single laser pulse made a crater 5 μm wide and 0.3 μm deep. In order to etch a continuous isolation trench we found that the positions of the laser spots had to be spaced as close as 2 μm.

Because the QWIP resistance increases with decreasing temperature, the defects become dominant or visible in the electroluminescent map only at low temperatures. This requires that the laser alignment with the defects and their removal by laser ablation are both performed *in situ* and at the QWIP operating temperatures (~77 K). Square isolation trenches as small as 10 μm × 10 μm were successful in isolating defects. Most of the square trenches were about 25 μm × 25 μm. This might be attributed to the variation in defect sizes. A completely shunted QWIP-LED device was successfully revived after the laser surgery, demonstrating that the laser ablation technique is a very effective tool to mitigate effects caused by crystallographic imperfections.

3.2.6 Substrate Removal Process

In order to reap all the aforementioned benefits associated with the transmissive QWIP-LED configuration, one must completely remove the GaAs substrate on which the device is grown. A complete substrate removal process was successfully demonstrated; the results were published elsewhere [4] and are summarized here:

3.2.6.1 Choice of optical adhesive

The choice of a suitable optical adhesive is the most important step towards achieving the substrate removal and high device performance. Requirements for the glue include the following:

(a) optical transparency at the LED emission wavelength (~850 nm);
(b) good long term performance at cryogenic temperatures (30-80 K);
(c) tolerance to thermal cycling and 400 K bakeout (i.e., resiliency which provides strain relief from temperature extremes);
(d) resistance to etchants and solvents;
(e) strong bond formation between the faceplate and GaAs; and
(f) good curing behaviors (e.g. low shrinkage).

Four different adhesives were evaluated: Summer Optical DC-90, Epotek 301 and 301-2AF, and Norland 83H. Only Norland 83H appeared to meet all the aforesaid requirements. The optical glue is a single component liquid adhesive which cures to a tough, hard polymer when exposed to UV light. In addition to UV light, heat can also be used to cure this one part adhesive. The heat-cure option is important when we consider bonding the device directly to a CCD chip to increase the LED external efficiency, since both GaAs and Si are opaque to UV light. The thermal cycling test also showed excellent resiliency of this type of glue. Heat curing above 80 °C, however, caused the device to cleave along the V-groove.

3.2.6.2 Controlling carrier/device parallelism and glue thickness

The second step towards the substrate removal is to polish the GaAs substrate so that about 50 μm of the substrate remains. The important requirement is that its thickness does not vary by more than ± 2 μm. In order to accomplish this, one must first protect the backside of the substrate during the front side processing of the device. The next step towards achieving the required accuracy is to ensure that, after bonding the device onto the fiber faceplate and before curing with UV or heat, the backside of the device substrate is parallel to the backside of the faceplate (i.e., the side facing the CCD). This was accomplished simply by using a Mitutoyo Digimatic Indicator to measure the combined thickness of the device – which includes the device, the glue, and the faceplate – at various points. This is followed by carefully adjusting the thickness of the glue using the tip of Digimatic Indicator to lightly press on the backside of the device so that a parallelism of ± 2 μm was achieved between the front and the back surfaces.

Another technique that we used to achieve a higher degree of parallelism and better control of the optical adhesive thickness was to use a contact mask-aligner to press the sample device against the carrier substrate during the bonding. The thickness could also be controlled by fine tuning the mask-aligner's vertical adjustment knob. A glue thickness of less than 1 μm was achieved using this technique. A good mask-aligner is designed to give excellent parallelism. The main motivation for maintaining a very thin optical adhesive is to reduce the effect of glue on the escape probability of LED light. This is particularly important when bonding the QWIP-LED directly to a CCD chip. The bonding strength of such a thin glue (i.e., < 1 μm) appeared to be still adequate; no delamination or debonding was observed during the thermal cycling test.

3.2.6.3 Avoiding bubble incorporation

Bubble incorporation in the glue must be avoided in order to prevent possible complications associated with stress induced by air bubbles shrinking and expanding during thermal cycling. The two-part adhesives such as Summer Optical DC-90 and Epotek 301 and 301-2AF have a greater chance of bubble incorporation because of an additional two-part mixing requirement.

3.2.6.4 Substrate polishing

We have limited the backside polishing of the substrate to ~50 μm in thickness in order to avoid possible damage to the device. We have actually thinned samples to about 20 μm, and still successfully wet etched off the remainder to the stop layer. However, none of these samples were fabricated into working devices.

3.2.6.5 Wet etch

The removal of the remaining ~50 μm substrate by wet-etch is a two-step process. A 45 s dip in 1:10 NH_4OH:H_2O solution ensured that surface oxides were completely removed before the citric acid etch. Experiments have shown that surface oxides can prevent uniform etching of the GaAs substrate by the citric acid and can lead to surface roughening.

3.2.7 CONCLUSIONS

Currently, the major obstacles that must be overcome in order to demonstrate a working QWIP-LED device with a reasonable performance are as follows:

- The designs of the top and bottom coatings. These are probably the most important hurdles that one must overcome. They directly affect the effectiveness of the 2-D grating coupler and the photon recycling, which in turn determine the performance of both the QWIP and the LED.
- The design of the LED and the photon recycling layer. This is probably the next most important step towards demonstrating a high external efficiency LED, which in turn affects the LED-to-CCD optical transfer efficiency.
- The design of the 2-D grating coupler. Several grating coupler designs were already tested and shown to work well before the substrate removal. For unknown reasons, the grating coupler failed completely when the substrate was removed.

On the other hand, V-groove coupler could be used instead of the 2-D grating now that a wafer with the up-side-down structure has been grown.

Several major hurdles have already been overcome. These include the hot-spot issue (solved by the laser ablation technique), the V-Groove influence on LED (solved by the up-side-down structure), the F/MIR attenuation at V-groove Facets (solved by the MgF_2 coating), and the substrate removal process.

3.3 QWIP-LED/CCD Optimization Research at EMS

3.3.1 Substrate Materials/Compatibility

Substrate materials that are transparent to the correct wavelengths of radiation are necessary to complete the coupling process. Matching of the coefficient of thermal expansion (CTE) of the substrate to the QWIP-LED is important to prevent tearing or cracking of the thin device upon cooling to cryogenic operating temperatures. For the transmissive design it is essential that the QWIP-LED be thinned down to its active dimension of ~ 4 μm after being bonded to a suitable substrate. This grinding and etching process requires that the rear surface of the substrate be parallel to the bonded QWIP-LED to prevent damage to the detector. NRC has had success in bonding the QWIP-LED to quartz and sapphire substrates at cryogenic temperatures using Norland 83-H optical adhesive.

The ideal option for maximum coupling efficiency is the direct bonding of the thinned QWIP-LED to the CCD detector. This option was discarded for several reasons. The main problem is that the QWIP-LED must be cooled to temperatures below 77K to minimize thermally generated background noise. Standard CCDs do not operate below this temperature due to charge carrier freeze-out. Therefore a thermal gradient of up to 30K must be maintained between the CCD and the QWIP-LED. Specially designed cryogenic CCDs can be envisioned, but the expense associated with such a development program would be difficult to justify within the QWIP-LED design paradigm of an affordable alternative to HgCdTe detectors. Furthermore, the thinning process as currently envisioned would entail a large risk of damage to the sensitive CCD detector. This risk could be mitigated by the implementation of an epitaxial lift-off procedure and adhesive-free Van der Waals bonding of the QWIP-LED thin film to a cryogenic-optimized CCD, but such a process would be well beyond the scope of this study.

The second best option in terms of coupling efficiency is a direct bond of the QWIP-LED to the fiber-optic faceplate, followed by back thinning of the device. The fiber-optic CTE is similar to that of quartz which means that previous NRC cryogenic bonding results can be accepted in place of further investigation on the stability of such a bond. The fiber-optic faceplate can be easily ground and polished at Lumonics

Optics (Nepean) to a specified tolerance of ~2.5μm, necessary for the delicate QWIP-LED back-thinning process. The process of bonding such faceplates to CCDs is also a well understood process at EMS due to heritage from several space-based scientific instruments as well as the current CALTRAC™ star tracker product.

3.4 Analysis of Options/Tradeoffs

3.4.1 Direct Bonding/Fiber Optic Faceplate

By eliminating any air gaps between the QWIP-LED and the CCD, a more efficient transfer of photons is made possible. This is because both the silicon-based CCD and the GaAs based LED have high refractive indices ~3 in the NIR region. In this way critical angle reflective losses can be minimized. The ideal solution for highest coupling efficiency would involve the epitaxial lift-off of the QWIP-LED from its GaAs substrate, followed by direct adhesive-free Van der Waals bonding to the bare CCD substrate. This option, discussed briefly in section 3.3.1 above, would eliminate the difficulty of getting the photons out of the high index substrate and into a low index transfer medium. This option was not pursued due to the high level of perceived risk and long lead time expected to perfect this delicate process. Ignoring the difficulty of mastering the epitaxial lift off and deposition of a 4μm thick crystalline semiconductor, this option would require that a CCD be produced which could operate at the necessary QWIP operating temperatures of 30-60 K. It is estimated that such a project could be accomplished through collaboration with a CCD manufacturer on a 2-3 year timescale with a budget of ~$1million CAD.

The next best course of action was to use direct adhesive-bonded contact with an insulating fiber-optic faceplate to achieve one to one imaging with high collection efficiency while maintaining the necessary thermal gradient for standard CCD operation. By mixing a small concentration of calibrated monodisperse index-matched microspheres into the adhesive prior to faceplate bonding onto the CCD, a bondline of constant thickness can be maintained. This is important for the resulting imaging performance of the detector, as it maintains a constant amount of blurring across the image as the photons emerge from the fiber-optic faceplate and spread out before encountering the CCD detection region.

To minimize reflective losses due to contrast and non-normal incidence onto the CCD, the refractive index of the glue line should be intermediate between that of the faceplate and the CCD. The refractive index of the faceplate core material is ~1.8, while that of the CCD is ~3. The highest available refractive index for commercial optical adhesives was 1.65 for Glue F from Stonehill Chemical in Ottawa, however the cryogenic performance of this glue was considered as poor. Standard optical adhesives have refractive indices near that of silica glass at ~1.56. The difference in normal incidence reflectivity due to the difference in refractive index between these

two glues is ~0.32%. The difference in fiber emission angle due to this index difference is also small (2.6° assuming fiber numerical aperture=1). Due to the relatively small gains afforded by the slightly higher index adhesive, it was decided that the cryogenic performance of the adhesive be used to rule out the Glue F as a viable option.

As long as the blurring from all the coupling elements is smaller than the diffraction limit of the incoming MIR radiation, no significant loss of resolution is expected. The resolution limit cannot be smaller than the wavelength of the incoming light, and will be limited by the design of the front-end imaging optics. For an optimized *f*/1 imaging system observing at 9 μm wavelength, the Rayleigh resolution criterion gives a characteristic blur spot of 22μm diameter. Theoretical results from NRC suggest that the image spreading contribution due to photon recycling inside the LED region of the QWIP will be limited to ~30μm. For the direct bond design, fiber diameters of ~4-6μm are used making the image transfer in this region blur-free. By choosing spacer balls with diameters <15μm, and indices of refraction matched to that of the glue to minimize scattering, the imaging performance should be maintained. In general, smaller ball diameters result in sharper image transfers. A summary of the expected image transfer blurring contributions is shown in Figure 3-2.

A bondline stress analysis was performed to predict the minimum spacer size to maintain adhesion at cryogenic temperatures as a function of adhesive choice. This analysis can be found in Appendix A. The results of this analysis show that spacers ≥10μm diameter should afford reasonable faceplate adhesion down to the necessary CCD operating temperature of ~80K as long as care is taken in the choice of adhesives. To verify these calculations, a cryogenic adhesive evaluation was performed in the CRESTech test chamber with various promising optical adhesives (Appendix B). The results of this test showed that both Glue D and Glue E were sufficient for cryogenic adhesion. Optical data was not available at 850nm for the Glue E, and the visual appearance of the cured gel suggested that it may not be completely transparent. In addition, the index of refraction of this low temperature gel was relatively low (~1.4) which would lead to a lower coupling efficiency. Therefore, the Glue D loaded with 15μm spacers was chosen as the best option for the faceplate to CCD bond.

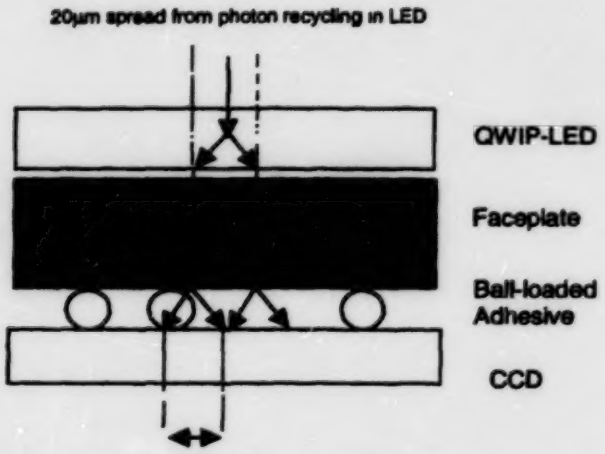

Figure 3-2 Image transfer blurring contributions for direct bond design

A thermal analysis was also performed to determine how best to minimize thermal gradients across the QWIP-LED and thus to eliminate thermally generated background fluctuations which could impact imaging performance. This procedure is detailed in Appendix C. The results of this analysis showed that with careful placement of thermal control elements and shaping of the fiber-optic faceplate, thermal gradients could be maintained across the QWIP-LED at less than 0.1°K.

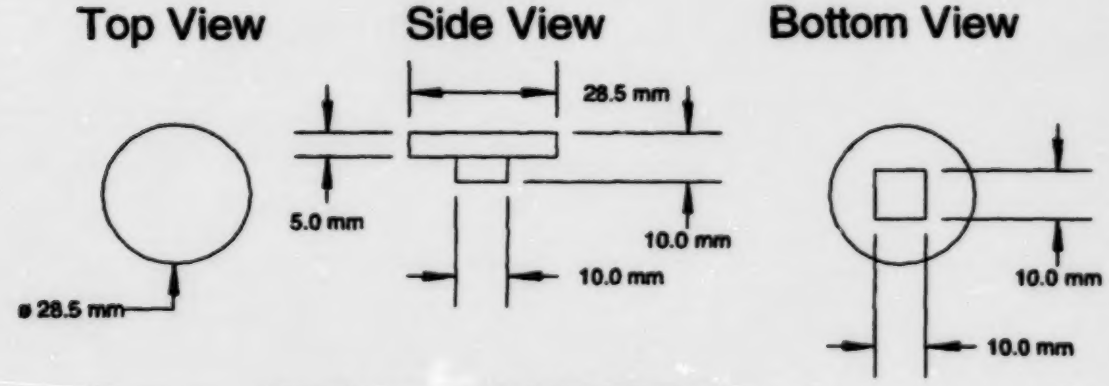

Figure 3-3 Fiber Optic Faceplate Design

Note that the fiber orientation runs from top to bottom in this sketch.

Two different faceplate designs were fabricated, one of which is shown Figure 3-3. The second design was identical except that the imaging fibers were extended from 1cm to a total length of 1.5cm top to bottom. This second option would increase the thermal isolation between the CCD and the QWIP thus decreasing the necessary cooling power, but would also tend to increase the stress on the CCD/faceplate bond due to the increase in mass. The large circular section on the top of the faceplate is where the QWIP-LED would be bonded. The imaging region would be centered on the faceplate so that emitted NIR photons could be transferred to the CCD. The large size is necessary so that there is sufficient contact between the cooling bracket and the partially-insulating faceplate so that the QWIP-LED temperature is uniform and can be held at the operating point of ~20K cooler than the CCD (~60K vs. ~80K). The final design is shown in Figure 3-4, mounted in its test jig for characterization.

3.4.2 Microgap

This option entails eliminating the transfer optics entirely, and bringing the CCD detector to within a few micrometers of the QWIP-LED surface. This is very difficult to implement in a robust design due to the necessary mechanical stability. The main drawback to this method is the large increase in reflected photons caused by the refractive index gradient between the QWIP-LED and air. This cannot be considered as an efficient transfer option due to the poor external LED efficiency upon emission to air.

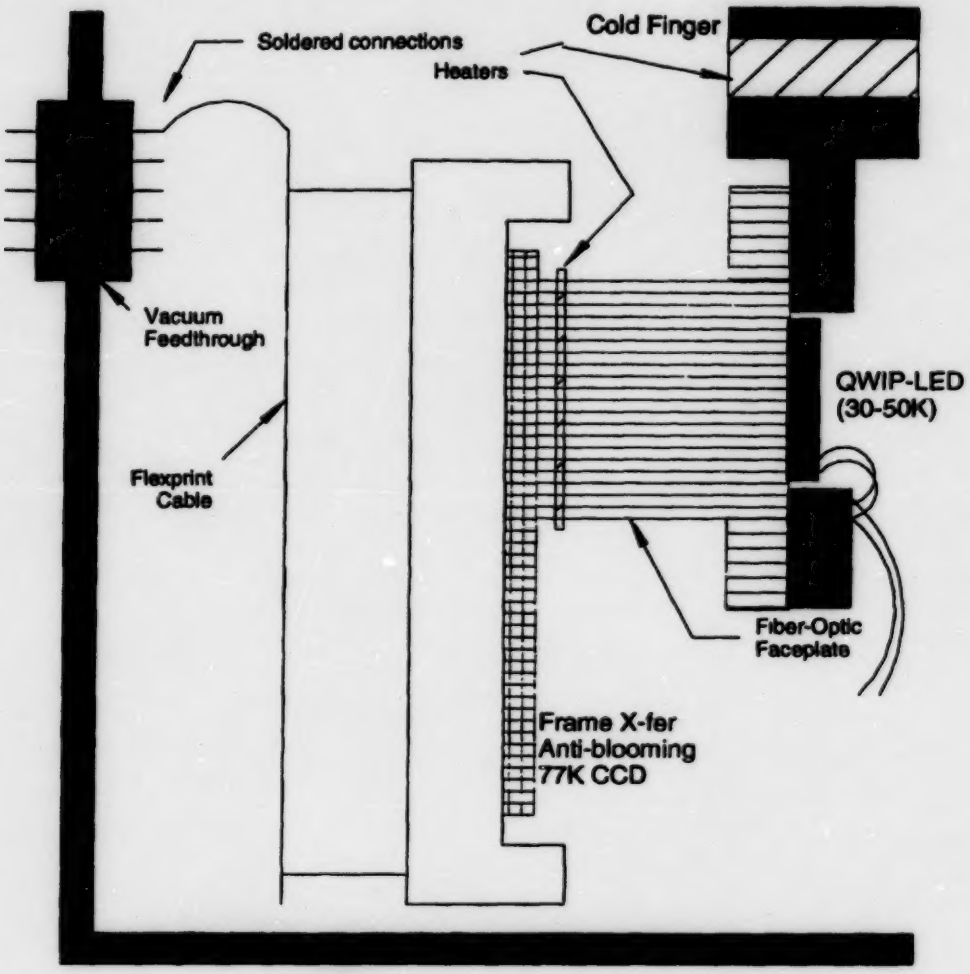

Figure 3-4a *Fiber Optic Direct Bond Design for QWIP-LED/CCD Coupling*

3.4.3 Non-Traditional Optical Solutions

Microlens arrays and Selfoc™ gradient index plates were investigated as potential new technologies which are known for high transfer efficiency. For pure light-collecting efficiency, these technologies are highly efficient due to their potential for close contact with the emitting source. For imaging applications, however, currently available products only offer transfer efficiencies comparable to ~f/1 optics. This is a

much lighter and more compact method than using conventional optics, but the coupling efficiency is not significantly improved. In addition to the unimproved transfer efficiency expected from these potential solutions, the alignment tolerances for incorporating a pixellated array of imaging quality are of comparable difficulty and expense to the indium bump bonding process commonly used in competing QWIP-multiplexers which achieve 100% transfer efficiency.

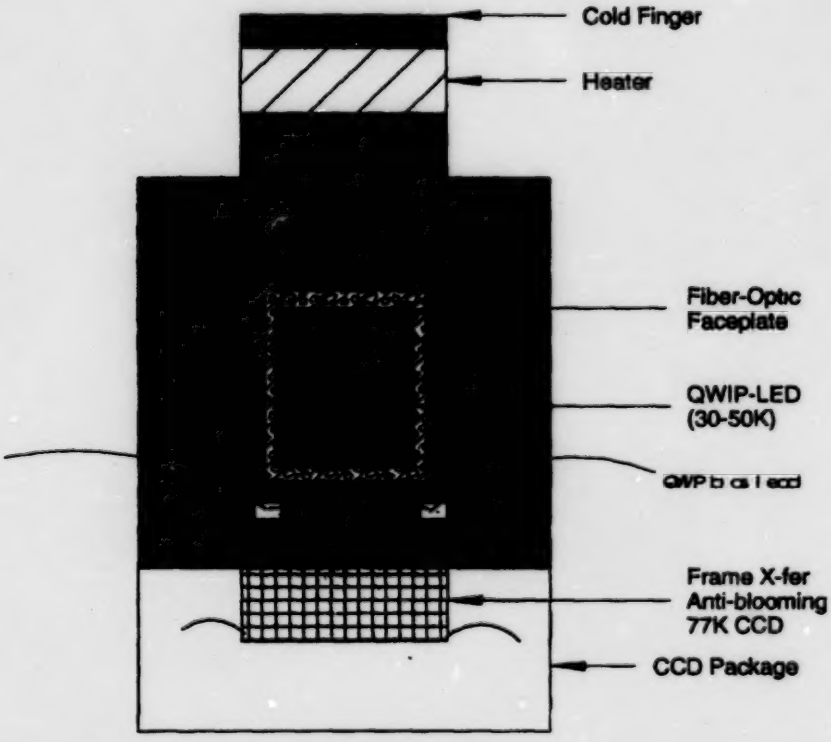

Figure 3-4b Fiber Optic Direct Bond Design for QWIP-LED/CCD Coupling

3.5 Bonding of Test Samples and Assembly Procedure

Bonding of fiber optic faceplates to CCDs and associated cryogenic testing is discussed in Appendix B. NRC test bonding of QWIP-LEDs to various substrates was described in section 3.2.6.1.

3.6 Testbed Design and Fabrication at CRESTech

This task included the alteration of a vacuum chamber for cryogenic characterization of CCDs and QWIP-LED/CCD assemblies, design and fabrication of a low thermal conductivity flexprint CCD preamplifier board, and training of an operator for the pre-existing Pulsed Instruments (PI) universal CCD readout electronics rack. The testbed is shown in *Figure 3-5*.

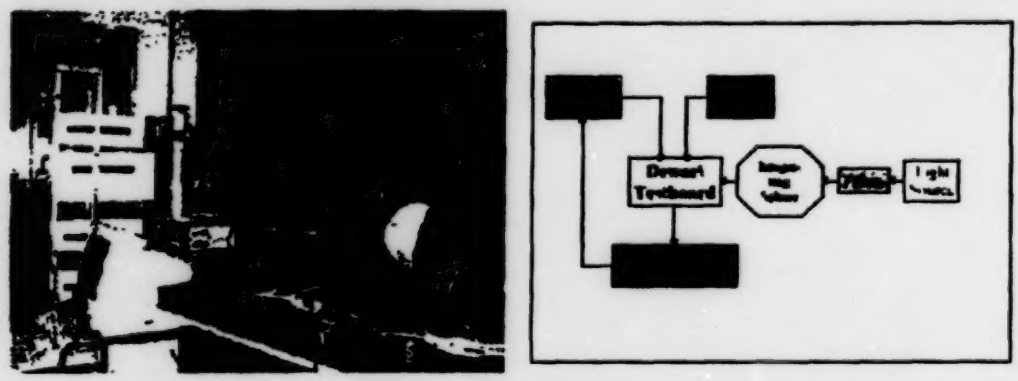

Figure 3-5 Cryogenic CCD Testbed at CRESTech

3.7 Test Procedure

3.7.1 Charge Transfer Efficiency

The method used to measure charge transfer efficiency is referred to as the Extended Pixel Edge Response [7]. The CCD is uniformly illuminated, then readout. With a non-perfect CTE, some charge is lost to overclocked pixels (ie. Trailing pixels that were not illuminated). The CTE can then be calculated as follows:

$$CTE = \frac{(S_i - S_d)^{\frac{1}{n}}}{S_i},$$

where
S_d = charge left in overclocked pixels
S_i = initial signal
CTE = charge transfer efficiency

n = number of transfers

3.7.2 Responsivity

Responsivity measurements were done in the 600-1000nm range. A calibrated photo-detector (ISTS-01318) was placed in front of the dewar window in order to measure light power density (W/cm^2). This, together with the pixel signal level from the CCD output and integration time is used to calculate the responsivity in V/(μJ/cm^2).

3.8 Acquisition and Characterization of CCDs

CCDs were chosen as the best option for the NIR imaging detector due to the maturity and familiarity of this technology, as well as the advantages associated with the adaptability of the CCD readout. It has been demonstrated that deep depletion back-thinned CCDs can achieve an excellent QE of ~0.85 at ~820nm as shown in *Figure 3-6*. This is as good as or better than most other available options in this wavelength region.

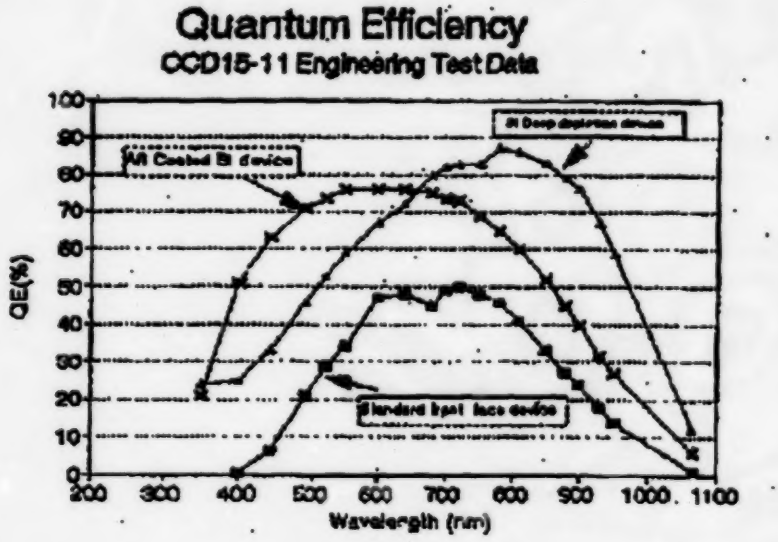

Figure 3-6 *Quantum Efficiency vs. Wavelength for Different CCD Types [8]*

It is commonly known [9] that standard unspecialized CCDs tend to operate well down to ~80K, below which point the charge carriers undergo freezeout and the charge transfer inefficiency (CTI) rises precipitously as shown in Figure 3-7.

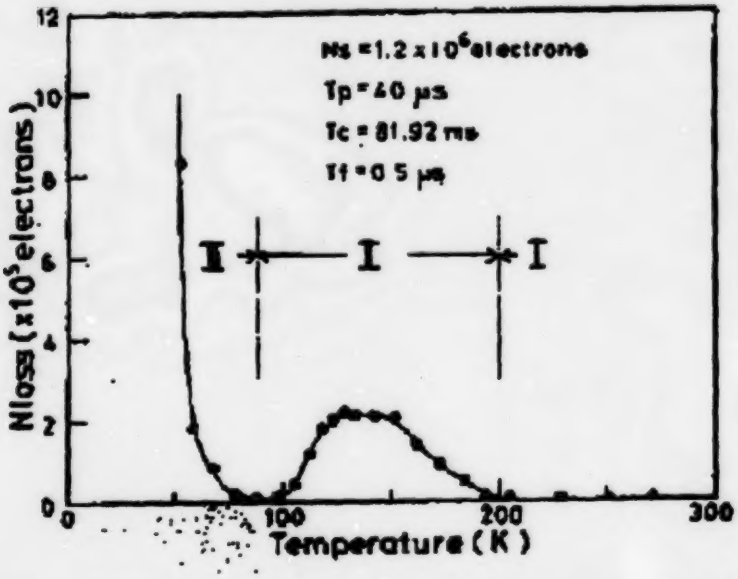

Figure 3-7a *0 - 300K Temperature versus Signal Loss due to CTI of Standard Buried Channel CCD [9]*

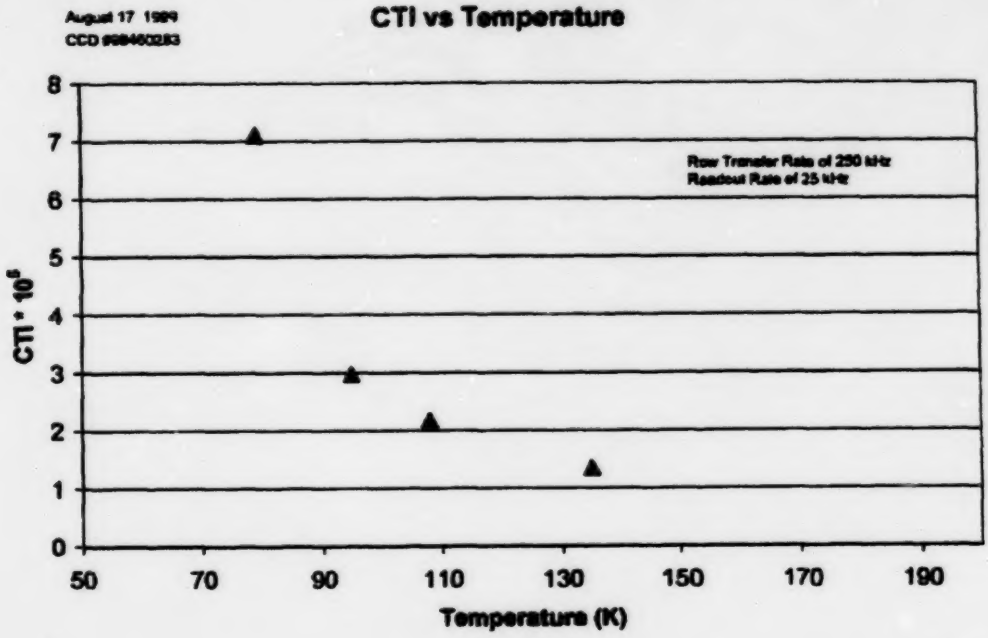

Figure 3-7b Measured CTI vs. Temperature for Dalsa CCDs Showing 80K Freezeout Effects

Due to QWIP-LED material defects in the devices being produced at NRC, it was thought to be essential that the chosen CCD incorporate anti-blooming protection to prevent 'hot spots' from ruining the image. Due to schedule and budgetary constraints it was decided to proceed to characterization with the Dalsa IA-D4-1024 CCD. This device is a 1024x1024 12μm pixel front-illuminated (lowest curve of *Figure 3-6*) frame-transfer device with vertical anti-blooming protection incorporated into the imaging region. Because it is not back-illuminated or deep depletion, this CCD is not an ideal device for maximum NIR absorption efficiency. The goal of the study, however, could still be achieved because the coupling efficiency of a high performance device can be directly extrapolated from the performance of this CCD assuming the actual QE is well characterized.

The readout rate chosen for operating these devices is limited at the upper end by the speed of the CCD readout circuitry (650kHz max. line shift on CRESTech PI readout electronics) and loss of charge transfer efficiency, and at the lower end by the saturation of the CCD pixel full well (1.1×10^5 e^- for the Dalsa CCD) and blurring of a moving image. A frame transfer device was chosen due to the high background signal expected from the QWIP-LED (see *Figure 3-8*). Practical image integration times are on the order of 10ms to prevent excessive image smearing during the frame transfer process. Assuming an optimized 16% transfer quantum efficiency (25% LED external

efficiency, 85% CCD QE, 75% faceplate transfer) for a QWIP which is sensitive to 9μm IR photons, this would require a QWIP operating temperature of <55K to allow proper CCD imaging to occur. Previous detector noise comparisons (QWIP-LED Application and Cost Estimate Study) show that the QWIP does not outperform standard HgCdTe IR detectors until the operating temperature drops below ~50K.

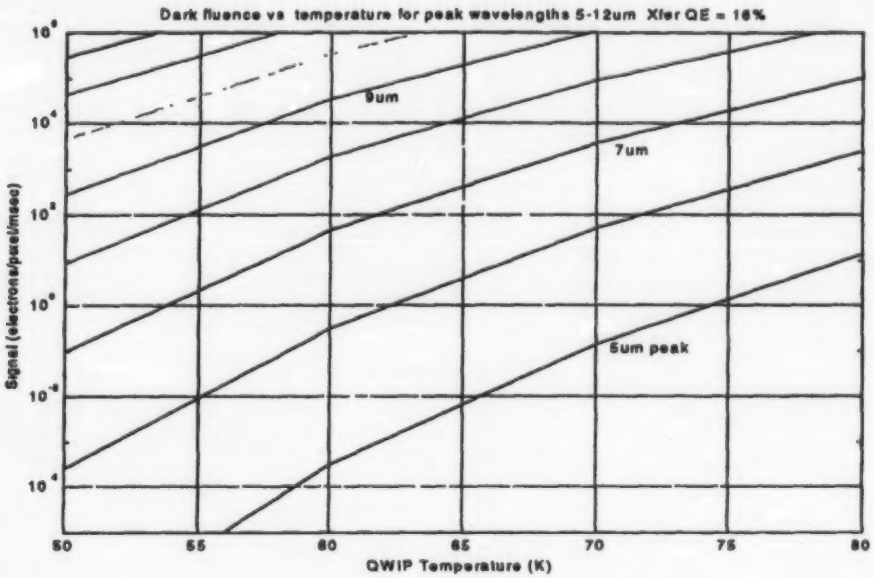

Figure 3-8 *Background Signal vs. Temperature and Waveband for QWIP-LED*

The ability to use frame transfer is very important for this application for a number of reasons. Most important is the ability to quickly shift the entire image under the storage shield at the line transfer rate of up to 650kHz. For 1024 pixels this corresponds to ~1.6ms. To prevent image smearing, the frame transfer time should be much smaller than the integration time. Once the image has been transferred under the store shield, the readout of the image can be implemented at the optimum rate to minimize CTI. CCD dark current at cryogenic temperatures is virtually zero, so the lower end of the pixel readout rate is given a practical limit by the desired frame update rate of the imager. The effects of readout rate on CTI are shown in *Figure 3-9*.

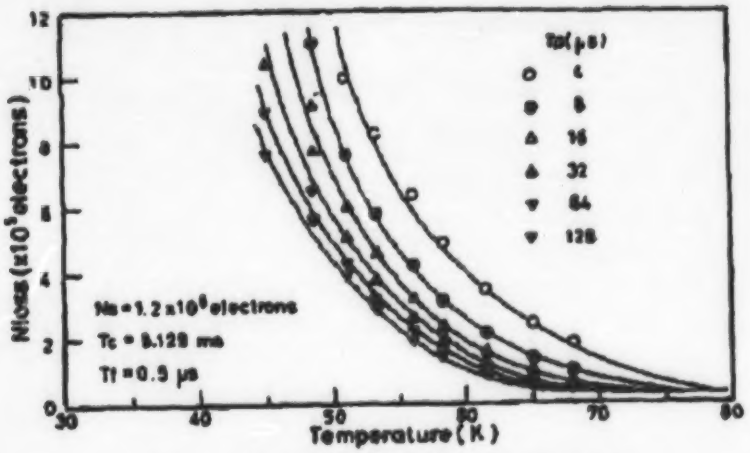

Fig. 7. Influence of T_p on N_{loss} in region III.

Figure 3-9a Signal Loss due to CTI vs. Temperature and Pixel Clock Period for Standard Buried Channel CCD [9]

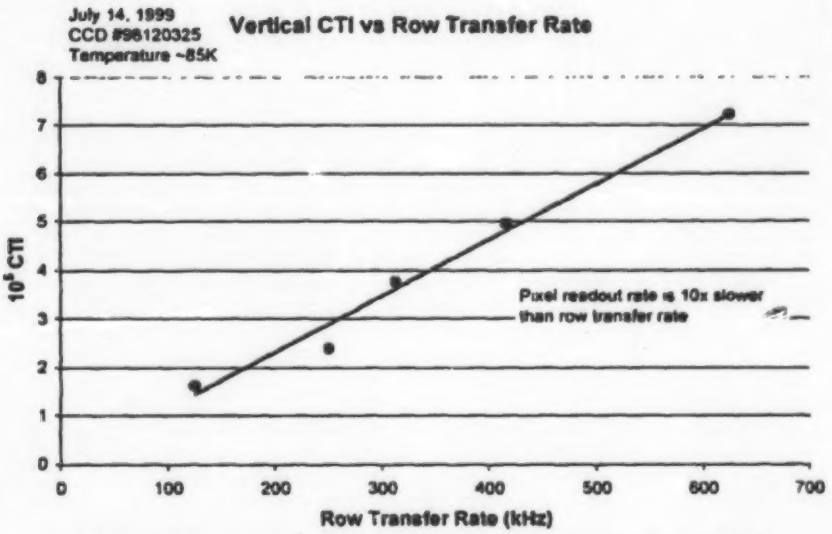

Figure 3-9b Measured Signal Loss vs. Transfer Rate at 85K

Figure 3-9a and Figure 3-9b show that the Dalsa CCDs achieve excellent values of CTI at 85K for readout rates <400kHz, and at 80K will operate at transfer rates of ~250kHz without significant loss of performance. A vertical shift CTI value of $7x10^{-5}$, as seen at 80K and 250kHz, corresponds to a maximum signal loss over the 2048 vertical transfers from the top of the image of

$$1-(1-7x10^{-5})^{2048} = 13.4\% .$$

This is not an ideal value, but it will allow reasonable image quality. For ease of readout implementation, the pixels on each row were read out at a sedate 25kHz rate, thus eliminating any further signal loss. At 1MHz pixel rate, it would take ~1 second to read an entire frame, but the CTI-induced losses at this rate may not be acceptable. For this reason it would be best that split frame CCDs with dual or quad outputs at opposite edges or corners be implemented for maximum frame rates in any future applications. This would allow doubling or quadrupling the readout rate without further impacting the CTI.

The operation of CCDs at cryogenic temperatures will have a secondary effect on responsivity in the LED wavelength region near 850nm. Because the crystal lattice of the silicon pixels will contract as the temperature decreases, the electronic properties of the material are noticeably affected. The practical effect of this temperature related shift in the band gap is a decrease in the long wavelength responsivity. This effect is shown in *Figure 3-10*.

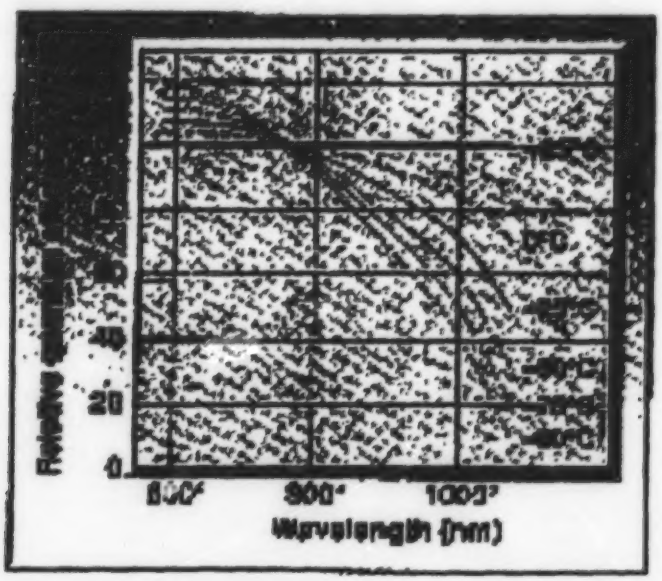

Figure 3-10a *Shift in Red Responsivity due to Cryogenic Cooling of CCD [10]*

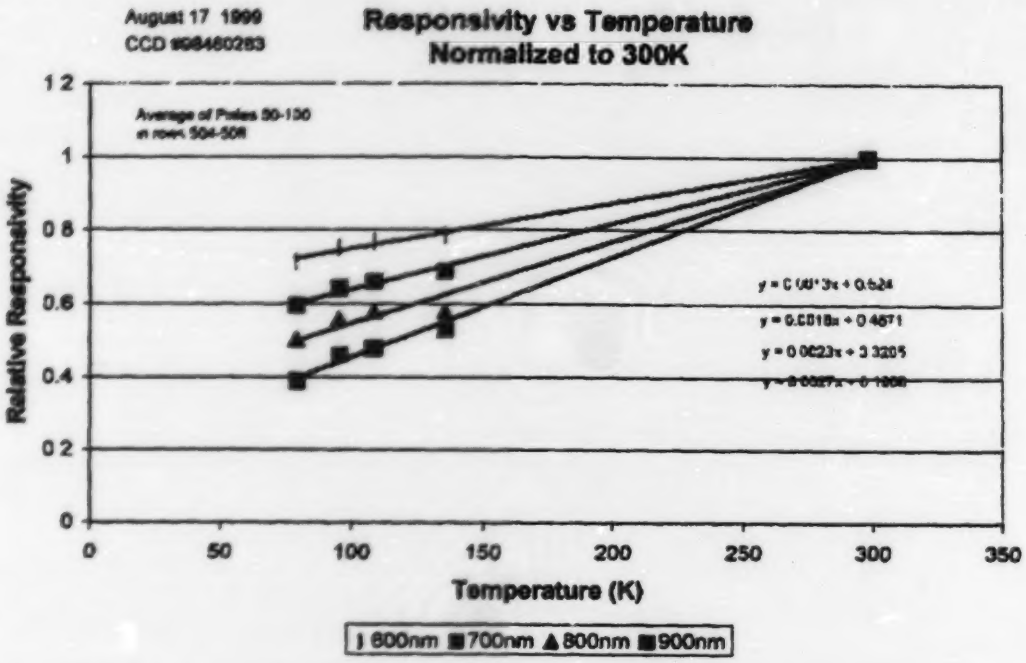

Figure 3-10b *Measured Shift in Dalsa CCD Responsivity vs. Temperature and Wavelength*

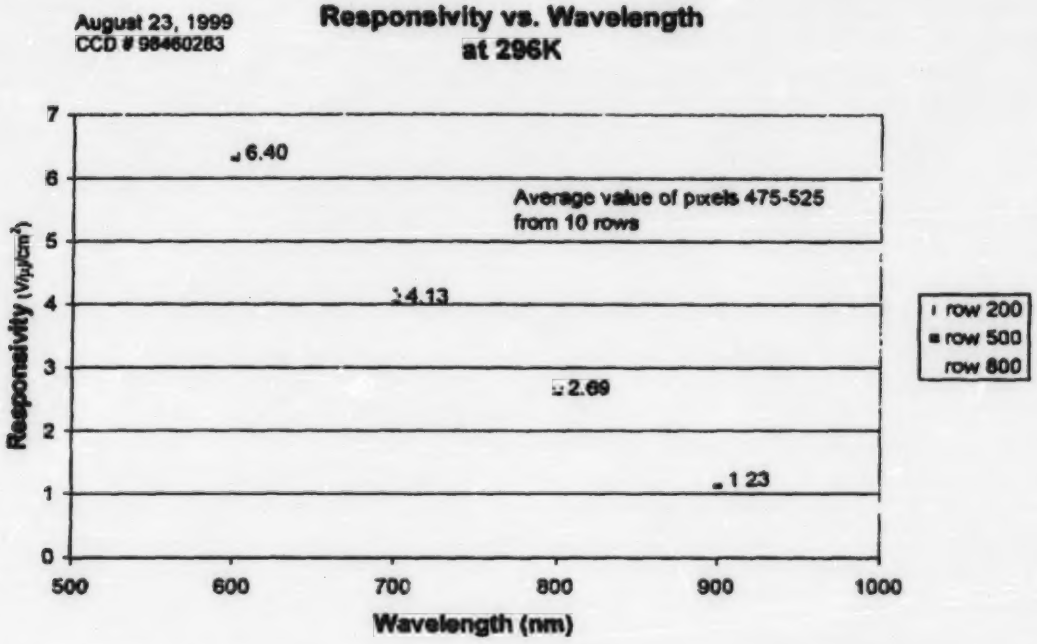

Figure 3-11 *Measured Responsivity of Dalsa CCD vs. Wavelength*

When the data from Figure 3-11 was converted to a quantum efficiency, the value in the 800-900nm region (<4%) was much lower than expected from commonly observed values for front illuminated devices (<40% Figure 3-6). The explanation for this deficiency was found in the vertical anti-blooming (VAB) structure used in this particular CCD. For Dalsa VAB devices, excess pixel charge is drained vertically into the substrate of the device. An unforeseen tradeoff in NIR quantum efficiency occurs when VAB is implemented. The VAB architecture establishes an additional potential barrier at approximately 3 μm pixel depth. Any additional charge which is generated in the buried channel flows across the barrier and is drained through the substrate. Due to the physical properties of silicon, red and NIR light will penetrate deeper than shorter visible wavelengths before being absorbed and freeing charge carriers. Because of the existence of the VAB potential barrier the collection of deep generated carriers, which would occur with relatively high efficiency in a standard device, is precluded.

4. Lessons Learned

Although this project failed to achieve its primary goal of creating a highly efficient QWIP-LED/CCD device, the attempt itself was highly instructive for each of the various study participants.

CRESTech was able to train highly qualified personnel in CCD theory and the use of PI universal CCD readout electronics. Device-portable procedures were created and tested for the characterization of scientific imagers over a range of temperatures and wavelengths. Experience was also created in the field of high speed pre-amp design and flexprint circuit prototyping.

EMS research into the field of cryogenic CCD operation as a result of this study has already been applied to phase A studies of scientific imagers for various astronomy and space science missions. Personnel gained experience in the use of CAD software tools for finite element analysis and thermal modeling. Extensive research in the field of semi-conductor physics, for interacting in a useful manner with NRC scientists, has resulted in the amassing of a higher level of expertise in the IR detector field, and increased awareness of issues currently faced by detector developers.

As a result of this study, it has become apparent that early projections about the cost, quality, and efficiency of pixelless QWIP-LED technology had been highly optimistic regarding critical implementation details. Unforeseen difficulties with the application of 'standard' LED and grating technologies to a non-standard device severely impacted the predicted efficiency for both absorption and emission.

EMS' research into the IR detector market allowed realistic comparisons to be made for expected applications showing that, in the near term and at the current rate of development, the QWIP-LED would not be an easily manufacturable competitive alternative due to cryogenic cooling requirements, unexplained material defects, and overall low efficiency. The competing QWIP-multiplexer which is now commercially available would have identical noise and cooling specifications with much higher efficiency at a comparable cost. Uncooled bolometric detectors would compete favourably for high signal terrestrial and earth-observing markets while at the high performance end, more efficient thin film HgCdTe detectors can now cover most wavebands of interest with much higher efficiency, thus out-competing QWIP-LED for space applications.

5. Conclusions

Based on the characterization data, it was determined that the overall system QE of a QWIP-LED/CCD device assembled using the Dalsa IA-D4-1024 CCDs would be quite poor, but should still be measurable to the necessary accuracy to determine the coupling efficiency of the direct bond method. The following calculations show the expected performance of various QWIP-LED/CCD systems based on current NRC projections of QWIP-LED performance. Note that a 50% coupling efficiency from LED to CCD was set as the original goal of this study to enable a 15% overall system QE. A pixelless device of this efficiency would be competitive with other IR detectors assuming the manufacturing cost remained low.

1. **Projected QE value for test system**

10% QWIP absorption × 80% LED internal × 15% LED coupling to faceplate × 90% faceplate to CCD × 2% CCD absorption
~0.02% overall QE

2. **QE of conventional optical relay with the same CCD**

10% QWIP absorption × 80% LED internal × 1% LED coupling to air × 10% lens to CCD × 2% CCD absorption
~0.0002% overall QE

3. **Projected QE value for hypothetical flight system with back-illuminated non-anti-blooming deep-depletion CCD ($$)**

10% QWIP absorption × 80% LED internal × 15% LED coupling to faceplate × 90% faceplate to CCD × 50% CCD absorption
~0.6% overall QE

Note that projected values for QWIP absorption and LED internal efficiency have not yet been reached.

References:

[1] E. Dupont, H.C. Liu, M. Buchanan, Z.R. Wasilewski, D. St-Germain, P. Chevrette, Proc. SPIE *3629* (1999) 155.

[2] K.K. Choi, The Physics of Quantum Well Infrared Photodetectors, pp. 189-200, World Scientific Publishing Co. (1997).

[3] J.Y. Andersson and L. Lundqvist, Appl. Phys. Lett. *59*, 857 (1991).

[4] S. Chiu, M. Buchanan, E. Dupont, C. Py, H.C. Liu, Infr. Phys. & Technol. *41* (2000) 51-60.

[5] R.J. Nelson and R.G. Sobers, J. Appl. Phys. *49*, 6103 (1978).

[6] S. Chiu, E. Dupont, DREO TR *1339* (December 1998), Defence Research Establishment Ottawa.

[7] J.D.Orbock *et al.*, "*Charge Transfer Efficiency Measurements at Low Signal Levels*," SPIE Proceedings, pg. 105-108. Feb. 1990, Santa Clara, California.

[8] EEV data

[9] Kimata, Denda, Yutani, Tsubouchi and Uematsu, "*Low-Temperature Characteristics of Buried-Channel Charge-Coupled Devices*", Jap. J. App. Phys., 22(6), p. 975, 1983.

[10] Mottola, A., and Denvir, D., "*Options increase for cameras cooled without liquid nitrogen*", Laser Focus World, *34*(5), p. 261, 1998.

APPENDIX A: Faceplate to CCD Bondline Stress Analysis

A.1 SCOPE

This document is intended to highlight the technical issues associated with the process of mounting the CCD fiber optic faceplate to the substrate material through the use of an adhesive bonding compound.

A.2 INTRODUCTION

There are a number of technical reasons for attempting to minimize the gap between the CCD substrate and the fiber optic faceplate. The aspect addressed in this document is the requirement to minimize this gap, thus limiting the scattering which occurs when the light incident on the faceplate is projected onto the CCD substrate. The difference in the coefficient of thermal expansion (CTE) between the fiber optic faceplate and the substrate material is the primary mechanical concern.

A.3 REFERENCE DOCUMENTS

[1] Product Specification, Philips Optics, SQ5360CCD

[2] Engineering Materials Selector 1991, Dec. 1990.

A.4 PROBLEM DEFINITION

The problem is to ensure sufficient mechanical strength of the bonded interface while minimizing the physical gap, h, as depicted in Figure A-1. The mechanical properties of the various materials are summarized in Table A-1. The physical dimensions of interest are the width (w) and length (l) of the faceplate, both 10mm.

Figure A-1 Schematic of the substrate/faceplate interface.

Table A-1 CTE Data for applicable materials.

Material	Faceplate	Silicon Substrate
CTE (10^{-6}) K^{-1}	6.55	4.67
Reference	RD 1	RD 3

Table A-2 Data for potential adhesives.

Property	Glue A	Glue B	Glue C	Glue D	Glue E
Cure					
η					
Elong. at Failure					
Elasticity Mod. (psi)					
Tensile Strength (psi)					
Transmission @825nm					
T_{max} (K as Specified)					
Phase Transition (K)					

Proprietary to IMS Technologies

A.5 ASSUMPTIONS

1. The center of the fiber optic faceplate is assumed to remain fixed while the faceplate and substrate expands uniformly about this point.
2. A temperature delta of 220°C from 25°C is sufficient to capture the entire range of operating conditions of the CCD.
3. The Young's modulus of the faceplate and substrate are much greater than that of the adhesive. Therefore all deformation can be assumed to be accommodated by the adhesive.
4. The Adhesive behaves in a linearly elastic manner with a Young's modulus as estimated in the following section.

A.6 CALCULATIONS

1) Diagonal Distance of Faceplate (d)

$$d = \sqrt{\left(\frac{l}{2}\right)^2 + \left(\frac{w}{2}\right)^2} = \sqrt{\left(\frac{10}{2}\right)^2 + \left(\frac{10}{2}\right)^2} = 7.1\text{mm}$$

2) Δl of Substrate to Faceplate Due to Thermal Expansion

$$\Delta d = d(\Delta cte)\Delta t = 7.1(6.55 - 4.67)\times 10^{-6}(220) = 0.0029mm$$
$$= 2.94\mu$$

3) Strain Induced in the Gap, h = 5μ

$$\varepsilon_{gap} = \frac{\sqrt{h^2 + \Delta d^2} - h}{h}$$
$$= \frac{\sqrt{5^2 + 2.94^2} - 5}{5}$$
$$= 0.160$$
$$= 16\%$$

4) Strain Induced in the Gap, h = 10μ

$$\varepsilon_{gap} = \frac{\sqrt{h^2 + \Delta d^2} - h}{h}$$
$$= \frac{\sqrt{10^2 + 2.94^2} - 10}{10}$$
$$= 0.042$$
$$= 4.2\%$$

5) Maximum Tensile Stress Induced

$$\sigma_{5\mu} = \varepsilon E$$
$$= 0.160(1.6E5)$$
$$= 25.6\,ksi$$

$$\sigma_{10\mu} = \varepsilon E$$
$$= 0.042(1.6E5)$$
$$= 6.72\,ksi$$

6) Stress Transformation to Max. Shear Stress

Assume : The elongation of the adhesive fibre between the corner of the faceplate and the substrate results in a state of pure tension along this fibre.

Therefore the max shear stress can be calculated from a Mohr's circle transformation as:

$\tau_{max,\,5\mu} = 25.6/2 = 12.8$ ksi

and

$\tau_{max,\,10\mu} = 6.725/2 = 3.4$ ksi

A.7 DISCUSSION

The Glue D has the highest elasticity modulus which was used to calculate the maximum tensile stress. For this particular adhesive, the tensile stress at failure is larger than that quoted for the 10μm gap. The other adhesives have somewhat lower elasticity moduli as well as lower tensile stress ratings. The important factor for comparison is the ratio between these numbers. For Glue D, the stress rating is 2.2% of the elasticity modulus. All the adhesives except for Glue A show higher ratios, suggesting that they will be successful in the 10μm gap case. For all of the adhesives, however, the quoted elongation at failure is larger than or at least equal to that in the 5μm case (step 3 above). This seeming inconsistency is likely due to the fact that the quoted elasticity moduli are not constants, and will vary with the applied strain. At low elongations or strain values, the moduli are probably much smaller. This suggests that 5μm would be achievable for all adhesives, while a 10μm gap would allow reasonable margin.

A.8 CONCLUSIONS

1. All adhesives studied should be sufficient for gap thicknesses down to 5μm over a 220K span of temperature.
2. Insufficient data were available for Glue E to determine in advance its expected behaviour.
3. Cryogenic testing is suggested to verify these conclusions.

APPENDIX B: Cryogenic Adhesive Trials for Faceplate Bonding

B.1 Assemble Fiber-Optic/CCD Bonding Jig

A pre-existing mechanical structure designed for the faceplate to CCD bonding process was altered to fit the CCDs and faceplates for this study. The bonding jig allows precise and stable positioning of the fiber optic onto the CCD surface while minimizing the chances of damaging the exposed bond wires which surround the CCD imaging area. Pre-cure of the adhesive would take place before the device is removed from the jig.

B.2 Pre-Set Testing

Microscope slides were used to test the amount of UV exposure necessary for a stable pre-cure of the UV-sensitive adhesives, as well as the amount of time necessary for pre-cure of the two part gel.

B.3 Adhesive Screening Test

Three electrically failed engineering test sample CCDs were acquired for the adhesive bonding trials. The procedure used for maximum adhesion is as follows:

1) Use standard optical techniques to clean faceplate bonding surface (methanol can be used here). Bake CCDs and faceplates in dry nitrogen environment @ 125°C for 24hrs to remove adsorbed water and organics. Be careful to maintain anti-static conditions using grounded aluminum foil for CCDs and faceplates.

2) Premix multi-part adhesives and mix in micro-spheres at ~1% by weight.

3) Degas adhesives in low vacuum ~20 minutes, cycling in air to break down bubbles.

4) Apply small drop to center of CCD using syringe (discard first drop as it usually contains bubbles).

5) Deposit faceplate with strong anti-static precautions and apply proper pre-cure. Never touch the pre-polished faceplate surface after bake-out is complete.

6) Remove device from bonding jig and complete the cure as directed.

7) Age the adhesive at 50°C for 12 hrs.

8) Slowly (~5°C/minute max.) cool device to 77K and observe results.

9) Warm to ambient and repeat step 8.

After the results were collated, the process was repeated using 3 working and 1 non-functional engineering grade CCDs to determine whether the bonding process was safe for working devices. UV-blocking effects of QWIP-LED on surface of faceplate were simulated with a piece of paper. UV exposures were lengthened to 6 hours from previous 20 minute cure time to see if sufficient transmission through the side of the faceplate would occur. Temperature of step 1 bakeout was set at 150°C by accident. All the results are shown in table B-1.

Table B-1 *Results of Adhesive Bonding Trials*

CCD Serial #	Adhesive (+ μballs)	Cure (+12hr @ 50°C aging)	Cryo-Observations
98160006 (dead)	Glue E		Faceplate stayed on
98160008 (dead)	Glue A		Faceplate fell off (potential handling error)
98460287 (dead)	Glue B		Smooth bond. Faceplate stayed on. Fissures at extreme bond edges. 2nd cycle adhesive separated from both CCD and faceplate.
970065 (dead)	Glue D		Smooth bond. Faceplate stayed on.
98120325	Glue C		Wrinkled and stressed bondline. Faceplate fell off upon warm-up.
98120322	Glue A		Dimpled bondline--glue on wire pads. Faceplate fell off upon 2nd warm-up cycle. Incomplete cure was evident.
970061	Glue E		Smooth bond. Faceplate stayed on.

Proprietary to EMS Technologies

All functional CCDs remained functional throughout the process. Minimum temperature reached was 85K measured on top of the ceramic CCD carrier.

APPENDIX C: Thermal Analysis

C.1 Thermal Analysis Procedure

A finite element model of the basic mechanical design of the QWIP-LED/CCD device was constructed using the NASTRAN CAD software package. Thermal and radiative properties of all materials and adhesives in the device were incorporated into the model. Where measurements or manufacturer's quotations were not available, reasonable estimates were used based on similar materials. Temperature dependence of the various parameters was also estimated or extrapolated as necessary. In addition to conductive couplings, a 77K black-body radiative enclosure was assumed. Also, a 4mW/cm^2 heat load was added to the QWIP to simulate projected LED recombination due to optical coupling losses in the 9μm QWIP waveband from a 300K scene at an f/1 view angle. CCD thermal loading conditions were varied to simulate 250kHz switching of the pixel capacitance as well as static bias load on the output FET. The flexprint connection to the CCD was modeled with the assumption that it was held at the intermediate temperature of 77K with a clamp to the radiation shield. The rear of the CCD ceramic package was also connected to the 77K thermal reservoir. The thermal collar, glued to the upper surface of the faceplate with conductive epoxy, was connected at one end to a 50K reservoir representing the cold finger. A thermal control braid was connected around the base of the fiber optic bundle just above the CCD interface and its properties were varied to maintain both the QWIP and CCD at their proper operating temperatures.

This arrangement is not unreasonable for a real cryocooled mechanical design. Most sub-77K cryocooling systems supply an intermediate temperature reservoir near 77K for the provision of a heat shield. This allows the device to operate at higher efficiency, since the heat lift available at very low temperatures is only a fraction of that at the intermediate point.

C.2 Results

The results of this analysis showed that the QWIP temperature is remarkably uniform for the conditions of the model. This is mostly due to the high lateral thermal conductivity of the GaAs layers and the conductive metallic surface contacts, combined with the large separation of the QWIP and CCD along the fiber-optic insulating bundle. This orientation results in most of the thermal gradients being supported along the optical axis of the fiber bundle. During CCD operation the capacitive heat load due to clocking the device at ~250kHz, under certain realistic assumptions, can exceed the cooling effect of the 50K QWIP through the faceplate. Because of this, it was found that the best use of the thermal braid around the base of the faceplate was for cooling. If a small thermal conductance was assumed from the 50K reservoir to this braid, the gradients along the faceplate were minimized, and the CCD was still able to maintain its temperature above 80K during operation. When the CCD is not in operation, the 77K thermal reservoir clamped to the lead wires and also to the rear of the CCD package are able to hold the CCD at an intermediate temperature above that of the 50K QWIP.

Figure C-1 shows the entire QWIP-LED and faceplate subassembly mounted on top of the rectangular CCD in its ceramic carrier. The square piece on the top of the unit represents the copper cooling collar, which is connected to the 50K reservoir at one end. This sits on top of the round portion of the fiber optic faceplate. In the center of the cooling collar is a rectangular hole where the QWIP-LED is to be located. Bias leads from the QWIP-LED would run from the contact pads onto ceramic wire bond pads located on top of the cooling collar.

The final comprehensive model showed a thermal gradient across the QWIP of only 0.02K (Figure C-2). This would result in a very uniform thermal background being emitted from the device. The CCD gradient was ~10°C from the imaging region beneath the square faceplate to far end of the storage and readout area (Figure C-3). Based on the data presented in Figure 3-9, this suggests that the CTI will improve as one moves further away from the cold image region. If the readout row is at ~88K as shown, this would make it feasible to do pixel readout at higher rates (~1MHz) than would be possible at 80K (~250kHz max.).

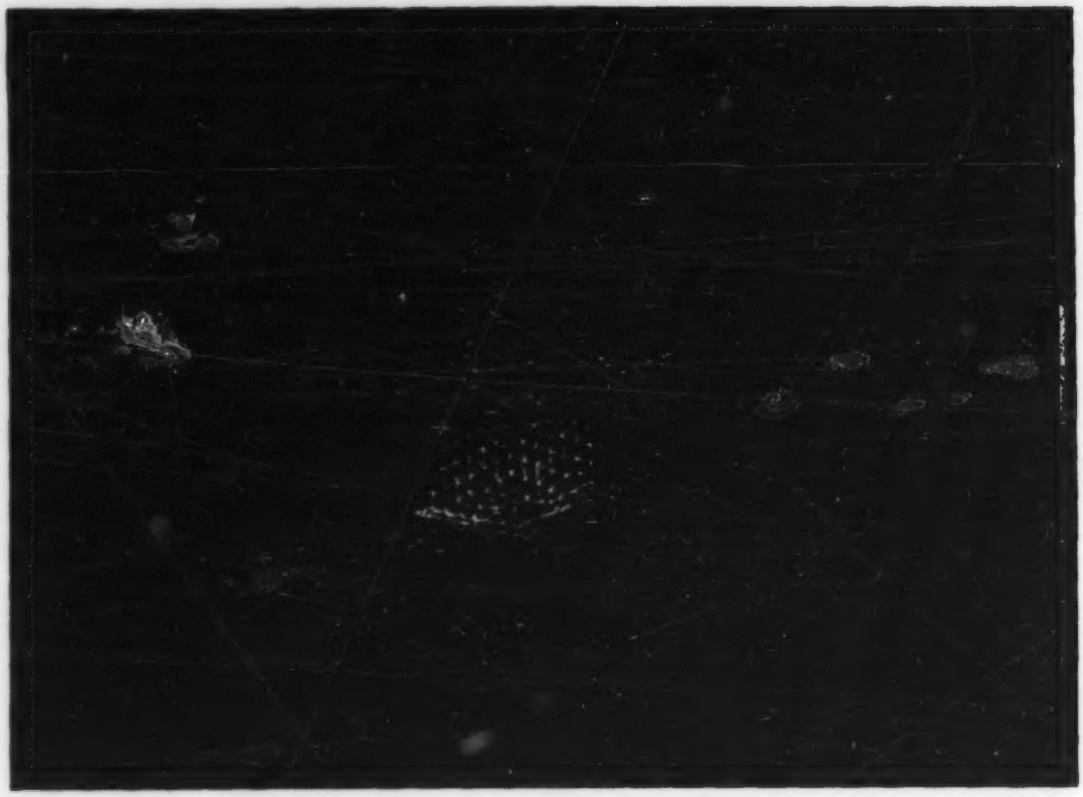

Figure C-1 QWIP-LED/CCD Thermal Analysis Results

Figure C-2 *Thermal Analysis Results for QWIP/LED Only*

Figure C-3 *Thermal Analysis Results for CCD Surface Only*

List of symbols/abbreviations/acronyms/initialisms

AFM	Atomic Force Microscope
CAD	Computer Aided Design
CCD	Charge Coupled Device
CTE	Coefficient of Thermal Expansion
CTE	Charge Transfer Efficiency
CTI	Charge Transfer Inefficiency
DND	Department of National Defence
DREO	Defence Research Establishment Ottawa
EL	Electro-Luminescence
EMS	EMS Technologies Canada
FIR	Far Infrared
IR	Infrared
LED	Light Emitting Diode
MIR	Mid Infrared
MUX	Multiplexer
NIR	Near Infrared
NRC	National Research Council
PI	Princeton Instruments
QE	Quantum Efficiency
QWIP	Quantum Well Infrared Photodetector
RIE	Reactive Ion Etching
SBIRS	Space Based Infrared System
TDI	Time Domain Integration
TM	Transverse Mode
UV	Ultraviolet
VAB	Vertical Anti-Blooming

UNCLASSIFIED
SECURITY CLASSIFICATION OF FORM
(highest classification of Title, Abstract, Keywords)

DOCUMENT CONTROL DATA

(Security classification of title, body of abstract and indexing annotation must be entered when the overall document is classified)

1. ORIGINATOR (the name and address of the organization preparing the document. Organizations for whom the document was prepared, e.g. Establishment sponsoring a contractor's report, or tasking agency, are entered in section 8.)

Defence Research Establishment Ottawa
3701 Carling Avenue
Ottawa, Ontario, Canada K1A 0Z4

2. SECURITY CLASSIFICATION (overall security classification of the document, including special warning terms if applicable)

UNCLASSIFIED

3. TITLE (the complete document title as indicated on the title page. Its classification should be indicated by the appropriate abbreviation (S,C or U) in parentheses after the title.)

QWIP-LED/CCD Coupling Study: Final Report (U)

4. AUTHORS (Last name, first name, middle initial)

Scott, Alan

Chiu, Shen

5. DATE OF PUBLICATION (month and year of publication of document)	6a. NO. OF PAGES (total containing information. Include Annexes, Appendices, etc.)	6b. NO. OF REFS (total cited in document)
December 2000	45	10

7. DESCRIPTIVE NOTES (the category of the document, e.g. technical report, technical note or memorandum. If appropriate, enter the type of report, e.g. interim, progress, summary, annual or final. Give the inclusive dates when a specific reporting period is covered.)

DREO Technical Report

8. SPONSORING ACTIVITY (the name of the department project office or laboratory sponsoring the research and development. Include the address.)

Defence Research Establishment Ottawa
3701 Carling Avenue
Ottawa, Ontario, Canada K1A 0Z4

9a. PROJECT OR GRANT NO. (If appropriate, the applicable research and development project or grant number under which the document was written. Please specify whether project or grant)	9b. CONTRACT NO. (If appropriate, the applicable number under which the document was written)
5EF12	

10a. ORIGINATOR'S DOCUMENT NUMBER (the official document number by which the document is identified by the originating activity. This number must be unique to this document.)	10b. OTHER DOCUMENT NOS. (Any other numbers which may be assigned this document either by the originator or by the sponsor)
DREO TR 2000- 101	

11. DOCUMENT AVAILABILITY (any limitations on further dissemination of the document, other than those imposed by security classification)

(x) Unlimited distribution
( ) Distribution limited to defence departments and defence contractors; further distribution only as approved
( ) Distribution limited to defence departments and Canadian defence contractors; further distribution only as approved
( ) Distribution limited to government departments and agencies; further distribution only as approved
( ) Distribution limited to defence departments; further distribution only as approved
( ) Other (please specify): DREO, DRDCIM, EMS Technologies

12. DOCUMENT ANNOUNCEMENT (any limitation to the bibliographic announcement of this document. This will normally correspond to the Document Availability (11). However, where further distribution (beyond the audience specified in 11) is possible, a wider announcement audience may be selected.)

Unlimited Announcement

UNCLASSIFIED
SECURITY CLASSIFICATION OF FORM

13. ABSTRACT (a brief and factual summary of the document. It may also appear elsewhere in the body of the document itself. It is highly desirable that the abstract of classified documents be unclassified. Each paragraph of the abstract shall begin with an indication of the security classification of the information in the paragraph (unless the document itself is unclassified) represented as (S), (C), or (U). It is not necessary to include here abstracts in both official languages unless the text is bilingual).

Many space-based imaging applications demand a sensitive, low noise long wavelength IR detector which is able to image a wide field of view in a short time. Quantum Well Infrared Photodetector (QWIP)-LED detectors offer the potential for large imaging area, and ultra-low noise operation when cooled to cryogenic temperatures (~30K). Due to these factors the QWIP-LED holds a significant advantage over conventional detectors. It is in the area of system efficiency, however, that current QWIP-LEDs are less competitive for low signal space applications. This study was a collaborative effort between EMS technologies, DND, CRESTech and NRC with a goal to design and implement a method to increase the efficiency of QWIP-LED systems.

As a result of this study, it has become apparent that early projections about the cost, quality, and efficiency of pixelless QWIP-LED technology were highly optimistic regarding critical implementation details. Unforeseen difficulties with the application of 'standard' LED and grating technologies to a non-standard device severely impacted the predicted efficiency for both absorption and emission.

EMS' research into the IR detector market allowed realistic comparisons to be made for expected applications and showed that, in the near term and at the current rate of development, the QWIP-LED would not be an easily manufacturable competitive alternative due to cryogenic cooling requirements, unexplained material defects, and overall low efficiency. The competing QWIP-multiplexer which is now commercially available would have identical noise and cooling specifications with much higher efficiency at a comparable cost. Uncooled bolometric detectors would compete favourably for high signal terrestrial and earth-observing markets while at the high performance end, more efficient thin film HgCdTe detectors can now cover most wavebands of interest with much higher efficiency, thus out-competing QWIP-LED for space applications.

14. KEYWORDS, DESCRIPTORS or IDENTIFIERS (technically meaningful terms or short phrases that characterize a document and could be helpful in cataloguing the document. They should be selected so that no security classification is required. Identifiers such as equipment model designation, trade name, military project code name, geographic location may also be included. If possible keywords should be selected from a published thesaurus. e.g. Thesaurus of Engineering and Scientific Terms (TEST) and that thesaurus-identified. If it is not possible to select indexing terms which are Unclassified, the classification of each should be indicated as with the title.)

Quantum Well Infrared Photodetector
Light Emitting Diode
Charge Coupled Device